Differential morphological changes in response to environmental stimuli in a fungal plant pathogen

Carolina Sardinha Francisco[a], Xin Ma[a], Maria Manuela Zwyssig[a], Bruce A. McDonald[a], Javier Palma-Guerrero[a]

[a]Plant Pathology Group, Institute of Integrative Biology, ETH Zürich, 8092 Zürich, Switzerland

Running Title: Pleomorphism in *Zymoseptoria tritici*

#Address correspondence to Javier Palma-Guerrero, javier.palma@usys.ethz.ch

ABSTRACT

During their life cycles, pathogens have to adapt to many biotic and abiotic environmental constraints to maximize their overall fitness. Morphological transitions are one of the least understood of the many strategies employed by fungal plant pathogens to adapt to constantly changing environments. We characterized the responses of the wheat pathogen *Zymoseptoria tritici* to a series of environmental stimuli using microscopy, transcriptomic analyses, and survival assays to explore the effects of changing environments on morphology and adaptation. We found that all tested stimuli induced morphological changes, with distinct responses observed among four different strains. The transcription analyses indicated a co-regulation of morphogenesis and virulence factors in *Z. tritici*. We discovered that *Z. tritici* forms chlamydospores and we demonstrate that these survival structures are better able to withstand extreme cold, heat and drought than other cell types. We also demonstrate that blastospores (the "yeast-like" form typically found only *in vitro*) can form from germinated pycnidiospores on the wheat leaf surface, suggesting that this morphotype can play an important role in the natural history of *Z. tritici*. Our experiments illustrate how changing environmental conditions can affect cellular morphology and lead to the formation of new morphotypes that can have a significant impact on both pathogen survival and disease epidemiology.

KEYWORDS

pleomorphism, environmental stimuli, cell morphology, plant pathogen, chlamydospore, virulence

INTRODUCTION

Fungi occupy a wide range of niches that can impose different environmental constraints on their growth, reproduction and survival. In response, fungi evolved the ability to detect and respond to different environmental stimuli in order to maximize their fitness (Brown, Cowen, di Pietro, & Quinn, 2017). One of the strategies that fungi employ to cope with diverse biotic and abiotic stimuli is to change their morphology (Lin, Alspaugh, Liu, & Harris, 2014; Mayer, Wilson, & Hube, 2013; Wang & Lin, 2012). For fungal pathogens, different morphotypes can play different roles during the host-pathogen interaction to improve the overall fitness. For example, hyphae may be the most appropriate morphology to cross physical barriers, colonize host tissue (Kumamoto & Vinces, 2005; Lin et al., 2014), and escape harmful environments generated by host defences (Brand, 2012; Kumamoto & Vinces, 2005). On the other hand, yeast cells (or "yeast-like cells") may be a better morphology to enable dispersal among host niches or between hosts and to increase the overall population size (Lin et al., 2014; Thompson, Carlisle, & Kadosh, 2011). The majority of fungal morphotype transitions occur between hyphal and yeast growth forms. Fungi with this ability are called dimorphic. Usually, they grow as saprophytic molds that live on dead organic matter and are facultative human pathogens, albeit dimorphism is also exploited by plant pathogens (Lin et al., 2014; Lübbehüsen, Nielsen, & McIntyre, 2003; Nadal, Garcia-Pedrajas, & Gold, 2008).

Some fungi can produce additional morphologies, including pseudohyphae and chlamydospores. Fungi that can produce more than two morphotypes are called

pleomorphic. Pseudohyphae are distinguished from true hyphae by constrictions that form at the septal junctions, leading to a loss in cytoplasmic continuity between mother and daughter cells (Veses & Gow, 2009). Though little is known about the ecological significance of pseudohyphae and their role during host infection, it was suggested that this morphotype facilitates foraging for scarce nutrients and increases motility in the host (Gancedo, 2001; Thompson et al., 2011). Chlamydospores are spherical, thick-walled cells formed on the tips of pseudohyphae or on distal parts of differentiated hyphae called suspensor cells (Noble, Gianetti, & Witchley, 2017). In contrast to pseudohyphae, chlamydospores are well-characterized and known to operate as long-term survival structures that can resist many environmental stresses (Couteaudier & Alabouvette, 1990; Lin & Heitman, 2005; McNeel, Kulkarni, & Nickerson, 1983; Noble et al., 2017; Son, Lee, & Lee, 2012). Pleomorphism has been observed in fungal pathogens of humans (Lin & Heitman, 2005; Miyaji, Sano, & Sharmin, 2003; Noble et al., 2017) and plants (Hoes, 1971; McNeel et al., 1983; Schade, Walther, & Wendland, 2003).

Genes controlling morphogenesis can be co-regulated with genes encoding virulence (Klein & Tebbets, 2007; Kumamoto & Vinces, 2005; Lin et al., 2014; Mayer et al., 2013; Nigg, Laroche, Landry, & Bernier, 2015; Thompson et al., 2011; Wang & Lin, 2012). The induction of virulence genes is usually associated with a specific morphotype. For example, certain virulence genes are expressed only during the yeast-phase of growth in *Histoplasma capsulatum,* while other virulence genes are expressed only during hyphal growth in *Candida albicans* (Brand, 2012; Edwards et al., 2013; Kumamoto & Vinces, 2005).

Zymoseptoria tritici is the most damaging pathogen of wheat in Europe (Fones & Gurr, 2015; Torriani et al., 2015) and an important pathogen of wheat worldwide. *Z. tritici* is considered a dimorphic fungus that grows either as blastospores (the “yeast-like” form) or as filamentous hyphae depending on the culture conditions. Though the role of blastospores in nature was unclear until now, hyphae are essential for penetrating wheat leaves through stomata (Kema, Yu, Frits, Shaw, & Baayen, 1996; Steinberg, 2015). The stimuli that induce morphological changes and the cell signaling pathways involved in morphological transitions remain largely unknown in this pathogen. Nutrient-rich media and temperatures ranging from 15°C to 18°C tend to induce blastosporulation (blastospore replication by budding) while nutrient-limited media and high temperatures (from 25°C to 28°C) tend to promote the blastospore-to-hyphae transition in the *Z. tritici* reference strain IPO323 (King et al., 2017; Motteram et al., 2011). Some genes affecting morphogenesis in *Z. tritici* were identified and functionally characterized. Most of these belonged to the mitogen-activated protein kinase (MAPK) or cAMP-dependent signaling pathways involved in extracellular signal transduction, regulating many cellular processes, development and virulence (Choi & Goodwin, 2011; Cousin et al., 2006; King et al., 2017; Mehrabi et al., 2009; Mehrabi & Kema, 2006; Mehrabi, van der Lee, Waalwijk, & Kema, 2006; Mehrabi, Zwiers, de Waard, & Kema, 2006; Mirzadi Gohari et al., 2014; Mohammadi et al., 2017; Motteram et al., 2011; Yemelin et al., 2017). However, the transcriptome signatures associated with specific morphologies were not reported until now.

In this study we aimed to characterize the morphological responses of *Z. tritici* to different environmental factors. We found that the fungus changed its morphology in response to all tested stimuli, although distinct responses were observed for four different strains sampled from the same geographical population. Transcriptional analyses showed a co-regulation of mycelial growth with expression of virulence factors. We discovered that *Z. tritici* forms chlamydospores both *in vitro* and *in planta*. We also found that pseudohyphae will form in some environments. We showed that blastospores can form by budding from pycnidiospores inoculated onto the surface of wheat leaves, demonstrating that this cell type can be produced under natural conditions. Based on these findings, we re-define *Z. tritici* as a pleomorphic fungus that produces four different morphotypes according to the associated environment.

Material and Methods

Fungal strains, environmental stimuli, and growth conditions. Four previously characterized *Zymoseptoria tritici* strains (ST99CH_1A5, ST99CH_1E4, ST99CH_3D1, and ST99CH_3D7, abbreviated as 1A5, 1E4, 3D1, and 3D7, respectively; (Croll, Zala, & McDonald, 2013; Zhan et al., 2005), were used in this study. 3D7 and 1A5 strains expressing cytoplasmic GFP (Kilaru, Schuster, Ma, & Steinberg, 2017) were provided by Dr. A. Sanchez-Vallet (Zala et al., 2018). All strains were grown in yeast sucrose broth (YSB; yeast extract 10 g/L and sucrose 10 g/L; pH 6.8). Depending on the tested environment, we used either YSB or a defined salts medium (Minimal Medium – MM, pH 5.8; (Vogel, 1956). Each strain was stored in glycerol at -80°C until required and then recovered in YSB medium incubated at 18°C for three days. For nutrient limitation

experiments, the cells were washed three times with sterile distilled water to remove any remaining nutrients prior to placing them into nutrient-limited conditions. Cell concentrations were determined by counting blastospores using a KOVA cell chamber system (KOVA International Inc., USA).

Effect of temperature on growth morphology. Blastospores of each strain were inoculated on YSB at a final concentration of 10^5 blastospores/mL. Three flasks were incubated at 18°C (as control) and three at 27°C for four days. An aliquot was taken from each flask at 8, 24, 48, 96, and 144 hours after incubation (hai) to monitor cell morphology by light microscopy using a Leica DM2500 microscope with LAS version 4.6.0 software. These experiments were repeated three times.

Effect of nutrient limitation on growth morphology. MM was used to monitor the transition in growth morphologies under different nutrient limitations. The effect of carbon depletion was assessed by adding each strain at a final concentration of 10^5 blastospores/mL into either regular MM, which contains sucrose as the main carbon source, or into MM without sucrose (C-depleted medium) and incubated at 18°C. The cell morphology was observed by light microcopy every 24 hours until 144 hai. The effect of nitrogen depletion was determined using MM lacking ammonium nitrate (NH_4NO_3), which is normally present in MM as the main nitrogen source. We compared the growth morphologies of cells growing in MM with and without ammonium nitrate by light microcopy during 96 hours of incubation at 18°C. The growth morphologies in both

nutrient-limited conditions were compared to the morphologies found in the nutrient-rich YSB. Experiments were repeated three times for each nutrient environment.

Effect of oxidative stress on growth morphology. Hydrogen peroxide (H_2O_2) was added into YSB at different concentrations (0, 0.5, 1, 2, 5, and 10 mM) to induce different levels of exogenous oxidative stress. Each strain was added to a final concentration of 10^5 blastospores/mL and incubated at 18°C. Morphological changes and cellular morphologies were observed by light microscopy at 72 hai. To determine whether a lower concentration of blastospores promotes a higher susceptibility to oxidative stress, we performed the same experiment using a final concentration of 10^3 blastospores/mL. These experiments were repeated twice.

Effect of pH on growth morphology. C-depleted medium (pH ~5.8) was used as a control. We also used a non-buffered C-depleted medium adjusted to be acidic (pH 4) or alkaline (pH 8) with 1 M HCl and 1 M NaOH, respectively. Three flasks containing C-depleted medium at the indicated pHs were inoculated at a final concentration of 10^5 blastospores/mL and maintained at 18°C. The pH was measured using a standard pH meter. Morphological changes were monitored by light microscopy at 8, 24, 72 and 168 hai. These experiments were repeated three times.

Effect of inoculum size on growth morphology. Flasks containing YSB or C-depleted medium were inoculated with a final cell density of 10^7 blastospores/mL, followed by a 10X serial dilution to a concentration of 10^3 blastospores/mL. Flasks containing C-

depleted medium were incubated at 18°C and flasks with YSB were incubated at 27°C. Cell morphology was determined every 24 hours using light microcopy over 144 hours of incubation. These experiments were repeated three times.

RNA extraction, library preparation, and sequencing. Flasks containing a final concentration of 10^5 blastospores/mL in YSB or C-depleted medium were incubated at 18°C to induce blastosporulation or mycelial growth, respectively. Total RNA was extracted by using TRIzol (Thermo Fisher Scientific, Waltham, Massachusetts) following the manufacturer's instructions. RNA quality was checked using a Qubit fluorometer (Thermo Fisher Scientific, Waltham, Massachusetts) and a TapeStation 2200 (Agilent, Santa Clara, California). Truseq stranded mRNA kit (Illumina Inc., San Diego, CA, USA) was used for library preparation, and ribosomal RNA was depleted by polyA enrichment. The quality and quantity of the enriched libraries were assessed using a Qubit fluorometer (Thermo Fisher Scientific) and TapeStation (Agilent). Libraries were sequenced on the Illumina HiSeq 2500 at 4 x 100 bp paired end reads.

Transcriptome mapping and quantification. The sequencing adapters and reads shorter than 15 bp were trimmed from raw Illumina reads using Trimmomatic v.0.36 (Bolger, Lohse, & Usadel, 2014) with the following settings: ILLUMINACLIP:TrueSeq3-PE.fa:2:30:10, LEADING:2 TRAILING:2, SLIDINGWINDOW:4:15 MINLEN:15. Filtered reads of each *Z. tritici* strain for the most common growth morphologies (blastospores and mycelial growth) were mapped against their respective genomes using Tophat v.2.0.13 (Trapnell, Pachter, & Salzberg, 2009). HTSeq-count v.0.6.1 was used to

196 calculate the gene counts (Anders, Pyl, & Huber, 2015). Mapped reads with more than
197 one reported alignment were excluded from further analyses. We applied the TMM
198 (trimmed mean of M values) method implemented in the Bioconductor edgeR v.3.12.0
199 package to normalize the gene counts and to calculate the differentially expressed
200 genes under each condition (Robinson, McCarthy, & Smyth, 2010; Robinson & Oshlack,
201 2010). Only genes with average counts per million reads per sample >1 for at least one
202 growth condition were counted as expressed genes. The Benjamin-Hochberg false
203 discovery rate (FDR) correction was used to adjust p-values based on the Fisher exact
204 test.
205
206 **Transcription profile analysis**. We generated the CPM (counts per million mapped
207 reads) values based on TMM-normalized library sizes obtained from the edgeR v.3.12.0
208 package (Robinson & Oshlack, 2010). Only genes with adjusted p-values of FDR≤0.01
209 were included in the analysis. The published transcriptomes of each strain during wheat
210 infection at 7 days post infection (dpi) (Palma-Guerrero et al., 2017) were used for
211 comparative analyses (datasets in NCBI SRA SRP077418). Only genes that were
212 significantly upregulated during both wheat infection at 7 dpi and in C-depleted medium
213 compared to YSB were considered to be mycelial growth-related genes. These genes
214 were used in further analyses. Specific transcriptome signatures were identified using
215 Venn diagrams based on the differentially expressed genes present in the *Z. tritici*
216 reference genome annotations (Grandaubert, Bhattacharyya, & Stukenbrock, 2015;
217 Plissonneau, Hartmann, & Croll, 2018) that were shared among all four strains under

each growth condition. We also used the published transcriptomes of different stages of wheat infection (Palma-Guerrero et al., 2017) to interpret the expression profiles of some genes under both axenic and *in planta* conditions. The log_2-transformed CPM values of those genes were plotted using the R package ggplot2 (Wickham, 2009).

Fluorescence microscopy to quantify chitin and lipids in different morphotypes. Blastospores of 1A5 were inoculated into YSB to a final concentration of 10^5 blastospores/mL and incubated at 18°C or 27°C to induce blastosporulation or chlamydospore-like formation, respectively. 1A5 was also inoculated at the same concentration into C-depleted medium and incubated at 18°C to induce hyphal growth. After four days of incubation, the resulting cells were harvested and fixed with 70% (v/v) ethanol for 30 minutes, followed by three washes with phosphate buffer saline (PBS). The cells were stained with 1 μg/mL of Calcofluor White (CFW – a chitin-binding dye) and 2.5 μg/mL of Nile Red (NR – a lipophilic dye) (both reagents from Sigma-Aldrich Chemie Gmbh, Munich, Germany) for 15 minutes. The stained cells were viewed with a Leica DM2500 microscope with LAS version 4.6.0 software, using a UV filter system for CFW consisting of an excitation filter at 340-380 nm and a long pass emission filter (>425 nm), and a red filter system for NR consisting of an excitation filter at 546-566 nm and an emission filter at 585-625 nm.

Transmission electron microscopy (TEM). Cells of 1A5 and 3D7 were collected after 4 days of growth in YSB at 18°C or 27°C. Pycnidiospores for each strain were harvested

from infected wheat plants. Samples were prepared using microwave-assisted fixation in 0.1 M cacodylate buffer (2.5% glutaraldehyde and 2% paraformaldehyde), using a PELCO Biowave (Ted Pella, California, USA), followed by embedding in 2% low melting temperature agarose (SeaPlaque Agarose, FMC Corporation, USA). A second step of microwave-assisted fixation was used after embedding in agarose. Before resin infiltration, the samples went through two steps of post-fixation, first in osmium tetroxide (OsO4) in 0.1 M cacodylate buffer and then in 1% uranyl acetate (UrAc), followed by a graded series of ethanol washes for dehydration (25%, 50%, 75%, 90%, and 100%). Samples were infiltrated with Spurr resin and polymerized at 60°C for 48 hours. Ultrathin sections (60 nm) were cut using the Leica Ultracut FC6 (Leica Microsystem, Vienna) and then transferred to formvar coated carbon grids, followed by post-staining with uranyl acetate and lead citrate. Micrographs were collected using a Morgagni 268 transmission electron microscope operating at 100 kV and using a CCD (1376x1032 pixel) camera.

Germination of chlamydospore-like cells and their survival under stress. Chlamydospore-like cells and blastospores of the 1A5 strain were harvested from YSB after 4 days of growth at 27°C or 18°C, respectively, and their concentrations were adjusted to ~10^5 cells/mL. 10 µL was spotted onto water agar (WA; 1% agar in water) and the plates were incubated at 18°C. Germ tube formation was checked at 0, 12, and 24 hours after inoculation by light microscopy.

To determine whether chlamydospore-like cells differ in their ability to survive environmental stresses compared to blastospores and pseudohyphae, we exposed $8x10^3$ cells/mL of each morphotype to different stresses, including drought and extreme temperatures.

For drought stress, 200 µL of each cell solution were spread onto Amersham Hybond™ N^+ nylon membranes (GE Healthcare Life Sciences, Chicago, Illinois) and dried in a sterile Petri dish placed on a sterile bench in a laminar flow hood. The Petri dishes were then placed into a sealed box containing anhydrous silica gel for 1, 3, 5, or 10 days. After the drought stress, the membranes were placed onto YMA plates (4g/L yeast extract, 4g/L malt extract, 4g/L sucrose, and 12g/L agar), incubated at 18°C and colony formation was monitored. Control membranes containing each morphotype were transferred directly to YMA plates without any drying treatments.

For cold stress, 300 µL aliquots of each cell solution were submerged into liquid nitrogen for 1, 2, or 3 minutes, and 200 µL of the thawed cell solution were spread onto YMA plates. Control samples were incubated at room temperature. For heat stress, 200 µL aliquots of each morphotype were incubated for 24 hours at 30, 35, or 40°C, followed by plating on YMA. Controls were kept at 18°C. YMA plates from control and treated samples were incubated at 18°C for seven days. Survival rates for each cell type were estimated based on the number of colonies formed after exposure to the stressful conditions compared to the number of colonies formed by the controls.

Plant infection assays. The susceptible wheat cultivar Drifter was used in all experiments. Plant growth conditions were described earlier (Meile et al., 2018). All infection assays used 16-day-old plants. For all four strains, blastospore suspensions produced after 3 days of growth in YSB at 18°C were filtered through two layers of cheesecloth and diluted to a final concentration of 10^6 blastospore/mL in 30 mL of sterile water supplemented with 0.1% (v/v) Tween 20. Spore suspensions were applied to run-off using a sprayer and the plants were kept for three days in sealed plastic bags, followed by 21 days in a greenhouse. Leaves with pycnidia were harvested and transferred to a 50 ml Falcon tube containing sterile water and gently agitated to harvest the pycnidiospores. Pycnidiospore suspensions were adjusted to a final concentration of 10^6 pycnidiospores/mL and a new batch of plants were inoculated as described above. The plants infected by pycnidiospores were used to observe the formation of chlamydospore-like cells on wheat plants.

To determine whether chlamydospore-like cells produce germ tubes and initiate hyhal growth after coming into contact with the host, we inoculated Drifter with chlamydospore-like cells from the 1A5 strain tagged with cytoplasmic GFP. Production of chlamydospore-like cells was induced using high temperature (YSB at 27°C) as described above. The suspension of chlamydospore-like cells was prepared and concentrations were standardized as described for blastospore infections. The inoculation procedure was the same except the inoculated plants were kept in plastic bags for only 24 hours.

306

307 To observe blastospore formation on the surface of wheat leaves, we inoculated plants
308 using blastospores of the 3D7 strain tagged with cytoplasmic GFP. At 21 dpi, GFP-
309 tagged 3D7 pycnidiospores were harvested and a new batch of plants was inoculated
310 using these pycnidiospores as described earlier. The inoculated plants were kept in
311 plastic bags at 100% humidity until they were examined for blastospores at 24 and 48
312 hai.

313

314 To observe formation of chlamydospore-like cells *in planta*, infected leaves from wheat
315 plants inoculated with pycnidiospores were harvested at 20 dpi. The infected leaves
316 were incubated in a humidity chamber for 24 hours, following by washes with sterile
317 distilled water to collect the released spores. The spore suspension was checked for the
318 presence of chlamydospore-like cells using a light microcope.

319

320 **Confocal microscopy of germinated pycnidiospores and chlamydospore-like**
321 **cells.** Confocal images were obtained using a Zeiss LSM 780 inverted microscope with
322 ZEN Black 2012 software. An argon laser at 500 nm was used to excite GFP
323 fluorescence and chloroplast autofluorescence with an emission wavelength of 490-535
324 nm and 624-682 nm, respectively. Plants inoculated with GFP-tagged 1A5
325 chlamydospore-like cells were checked at 24 hai to observe germination of the
326 chlamydospore-like cells. The same confocal settings were used to determine whether
327 pycnidiospores produced blastospores on the leaf surface. Wheat plants inoculated with
328 GFP-tagged 3D7 pycnidiospores were checked at 24 and 48 hai.

RESULTS

High temperature induces distinct morphologies in different *Z. tritici* strains. We exposed four different *Z. tritici* strains to high temperature. Three of the strains (1E4, 3D1, and 3D7) differentiated to filamentous growth at 27°C (Figure 1). The timing of the hyphal transition ranged from 8 hai for 1E4, to 24 hai for 3D1 and 3D7 (Figure 1B and C). Branching and hyphal elongation were frequently observed at 48 hai (Figure 1D, E, and F). Surprisingly, high temperature promoted the formation of two new morphologies, with appearances matching pseudohyphae and chlamydospores, in the 1A5 strain (Figure 1E and F). These morphologies were not reported previously for this well-studied pathogen. Chlamydospore-like cells were found for all strains at 144 hai (Figure 1F). Cellular differentiation from blastospores to pseudohyphae began in 1A5 at 24 hai, resulting in a series of conjoined elongated cells, characteristic of pseudohyphae (Veses & Gow, 2009) (Figure 1C). We also observed several swollen cells at 24 hai that we believe represent the initial differentiation from blastospores into chlamydospore-like cells (Figure 1C), but the complete differentiation occurred between 48 and 96 hai (Figure 1D and E). Chlamydospore-like cells were observed at the ends of pseudohyphae or distal parts of filamentous hyphae (Figure 1F). Chlamydospore-like cells that were detached from suspensor cells were also found (data not shown). Blastospores incubated in YSB at 18°C continued to replicate only as blastospores via blastosporulation and were used as controls (Figure 1A).

A nutrient-limited environment promotes filamentous growth. Carbon- or nitrogen-depleted medium promoted hyphal growth in all four strains (Figure 2 and Supplementary Figure S1). In a carbon-depleted environment, cellular differentiation occurred after 24 hours of incubation (Figure 2). At 24 hai, hyphal formation was observed with the first hyphal branch formed terminally (1A5 and 3D1) or laterally (1E4 and 3D7) (Figure 2B). Hyphal elongation and branching continued at 48 and 72 hai (data not shown). By 144 hai mycelial growth was predominant, with frequent anastomosis events among hyphae (Figure 2C). In MM with sucrose, all strains grew as a mixture of blastospores and hyphae, with blastospores budding from filamentous hyphae, showing that the morphological transition is bidirectional (Supplementary Figure S1C). Blastospores incubated in YSB continued to replicate only as blastospores via blastosporulation (Figure 2A).

In nitrogen-depleted media, three strains (1A5, 3D1, and 3D7) initially formed hyphae from one apical end, generating the first and second hyphal elongations within 72 hai (Supplementary Figure S1B). 1E4 responded most quickly to a low nitrogen environment, with hyphae forming at 24 hai (Supplementary Figure S1A) and a network of filamentous hyphae formed at 72 hai (Supplementary Figure S1B). In regular MM all strains grew as a mixture of morphotypes (Supplementary Figure S1C). The hyphae induced under both carbon and nitrogen limitation (Figure 2 and Supporting information Figure S1) were thinner than those produced by high temperature (Figure 1).

373 **Oxidative stress induces morphological changes in some strains**. At a high initial
374 cell density (10^5 blastospores/mL), the presence of H_2O_2 stimulated hyphal growth in
375 1E4 up to a concentration of 5 mM (Supplementary Figure S2). 1A5, 3D1, and 3D7
376 continued to replicate as blastospores, but there was a substantial reduction in
377 blastospore formation starting at 5 mM H_2O_2 (Supplementary Figure S2). To test
378 whether a lower concentration of blastospores would change sensitivity to oxidative
379 stress, we inoculated flasks with 10^3 blastospores/mL. After 72 hours of incubation in 0.5
380 mM H_2O_2, strains 1E4 and 3D1 showed apical and lateral hyphal branching
381 (Supplementary Figure S3), but both strains continued to form blastospores. At 1 mM,
382 blastospores from 1E4, 3D1, and 3D7 developed into a mixture of pseudohyphae and
383 regular hyphae (Supplementary Figure S3). The higher sensitivity at low cell densities
384 suggests that the exogenous H_2O_2 was more rapidly degraded by secreted
385 hydroperoxidase proteins (catalases, peroxidases and catalase-peroxidase) when cell
386 densities were 100X higher. The 1A5 strain did not switch to a different morphotype at
387 any H_2O_2 concentration, continuing to replicate as blastospores (Supplementary Figure
388 S3). Starting at 2 mM H_2O_2, none of the strains changed their morphology
389 (Supplementary Figure S3) and blastosporulation ceased (from 5 mM to 10 mM),
390 suggesting a cytotoxic effect of H_2O_2 at these concentrations.
391
392 **Alkaline pH inhibits the morphological transition to hyphae.** Because we observed
393 that *Z. tritici* does not change the pH of its medium, we inoculated blastospores into a
394 non-buffered C-depleted medium. All four strains switched to hyphal growth when
395 incubated at pH 5.8 (control) for 168 hours (Supplementary Figure S4A; Figure 2C).

Blastospores incubated at pH 4 also switched to filamentous hyphae, with no differences visible compared to the control samples (Supplementary Figure S4B). The morphological transition to hyphae was absent in all tested strains when incubated at pH 8 (Supplementary Figure S4C), but we noticed that the cellular compartments of the blastospores were highly vacuolized in all strains (Supplementary Figure S4C).

Inoculum size effect suggests that quorum sensing may affect morphology. We incubated all four strains at five cell densities in two growth conditions shown to induce hyphal growth. After 144 hours of incubation in C-depleted medium, we observed that morphology was independent of cell density for all four strains up to a concentration of 10^5 blastospores/mL (Supplementary Figure S5A), with most of the blastospores switching to hyphal growth and forming mycelial colonies. However, when the initial cell density was $\geq 10^6$ blastospores/mL, we observed a substantial reduction in the blastospore-to-hyphae transition and in hyphal length. No hyphae formed for 3D1 and 3D7 at initial cell densities of 10^7 blastospores/mL, and they were clearly reduced for 1E4 and 1A5 (Supplementary Figure S5A).

In YSB at 27°C we also found that initial inoculum size affected cell morphology (Supplementary Figure S5B), though there were more pronounced differences among strains in this environment. At 144 hai, starting from the lowest initial cell density (10^3 blastospores/mL), we observed pseudohyphae formation in 1A5, 1E4, and 3D1, and a mixture of pseudohyphae and chlamydospore-like cells in 3D7. At an initial density of

418 10^4 blastospores/mL, the same phenotypes were found, except that 3D1 formed apical
419 and lateral hyphae. Intermediate initial cell densities (10^5 and 10^6 blastospores/mL)
420 promoted hyphal growth for 1E4, 3D1 and 3D7, but the 3D7 strain grew as a mixture of
421 mycelium and chlamydospore-like cells at 10^6 blastospores/mL. The increase of the
422 inoculum size to 10^7 blastospores/mL induced formation of chlamydospore-like
423 structures in 1E4 and 3D1, and a transition from blastospores to pseudohyphae and
424 chlamydospore-like cells in 3D7. 1A5 was not able to switch to hyphae under high
425 temperatures in any of the initial cell densities (Supplementary Figure S5B). The overall
426 pattern of cell density dependence shown here suggests that a quorum sensing
427 molecule may be controlling the morphological transition, as has been reported for other
428 pleomorphic fungi (Hornby et al., 2004; Hornby et al., 2001; Wedge, Naruzawa, Nigg, &
429 Bernier, 2016).
430
431 **Mycelial growth is co-regulated with virulence-related genes.** Aiming to identify
432 genes associated with mycelial growth in nutrient-poor environments, we analyzed the
433 transcriptome signatures associated with blastospore and mycelial growth. The total
434 number of sequencing reads and mapped reads per strain under different growth
435 conditions is given in Supplementary Table S1. A total of 4888, 5296, 5323, and 6003
436 genes were differentially expressed among all tested conditions in 1A5, 1E4, 3D1, and
437 3D7, respectively. On average, 24% and 25% of the genes were upregulated during
438 blastospore and mycelial growth, respectively.
439
440 The upregulated genes shared among all four strains for each morphology were

441 selected based on pairwise comparisons. These genes were then analyzed using a
442 Venn diagram. Two distinct sets of 134 genes shared among the four strains were
443 identified in both comparisons. The first set is composed of genes that were upregulated
444 during blastospore growth: these genes were upregulated in YSB compared to C-
445 depleted medium, and were upregulated in YSB compared to the wheat infection, FDR
446 ≤0.01 (Supplementary Figure S6A and Table S2). The second set consists of genes that
447 were upregulated during mycelial growth: these were upregulated in C-depleted medium
448 compared to YSB, and were upregulated in wheat infection compared to YSB, FDR
449 ≤0.01 (Supplementary Figure S6B and Supplementary Table S3). For both comparisons,
450 the sets of genes that do not overlap represent genes with a strain-specific expression
451 profile.
452
453 Among the 134 shared genes that are significantly upregulated during blastospore
454 growth, 20% are annotated as *hypothetical proteins* (Figure 3A; Supplementary Table
455 S2). The remaining 107 genes are divided in fourteen biological process categories, with
456 *metabolism* the most represented term (44%). This category was composed mainly of
457 non-secreted enzymes, including oxidoreductases (n=11), dehydrogenases (n=8),
458 hydrolases (n=7), and transferases (n=9) (Figure 3A). No enrichment was found for any
459 other category. However, seven genes from other categories were already described in
460 other fungi to be involved in blastosporulation (Supplementary Table S4). As expected,
461 genes related to vegetative blastospore growth were highly expressed in nutrient-rich
462 medium - the environment most conducive for this morphotype (Supplementary Figure

S6C).

Among the 134 genes that were upregulated in all strains during mycelial growth, we observed an enrichment of secreted proteins (32%) known to be associated with fungal virulence, including *candidate effectors* (small secreted proteins - SSPs), *secreted proteases*, *secreted glycosidases*, *secreted chloroperoxidases, cell wall hydrolases, hydrophobins,* and *hydrophobic surface binding proteins* (Figure 3B and Supplementary Table S3). Overall, these virulence-associated genes were upregulated in C-depleted medium and during all stages of plant infection, albeit with a reduction in expression during the saprophytic phase of infection (at 28 dpi). The peak of expression preceded the first visual symptoms of infection, at 12 dpi for 1A5 and 3D7, and at 14 dpi for 1E4 and 3D1 (Supplementary Figure S6D), as previously reported for some of these gene categories (Palma-Guerrero et al., 2017). These patterns suggest that mycelial growth is co-regulated with the expression of genes relevant for virulence even in the absence of the host. We also detected the upregulation of six genes related to cellular morphogenesis (Supplementary Table S5). The transcription profiles of these genes showed an upregulation in both mycelial growth conditions (C-depleted medium and plant infection at 7 dpi) with the peak of expression occurring at 7 dpi for all four strains (Supplementary Figure S6E).

Chlamydospore-like cells are produced by *Z. tritici*. We observed the formation of structures with the same morphology as chlamydospores that had never been previously reported in *Z. tritici*. We aimed to determine whether these chlamydospore-

like cells had properties associated with chlamydospores in other fungi. Chlamydospores are known to be survival structures that have thicker cell walls and a high content of lipid droplets (Bottcher, Pollath, Staib, Hube, & Brunke, 2016). We stained the different morphological cell types of 1A5 with the chitin-binding dye Calcofluor White (CFW) and the lipid droplets dye Nile Red (NR) to measure these properties. The intensity of CFW fluorescence was higher in chlamydospore-like cells (Figure 4A, B, and C) compared with blastospores, hyphae, and pseudohyphae that exhibited a weaker fluorescence for CFW (Figure 4). NR staining revealed that chlamydospore-like cells had a high content of lipid droplets, which was also observed for blastospores and pseudohyphae. On the contrary, hyphae showed a lower lipid droplet content than spores, with the exception of the hyphal branching zones (Figure 4) as has been reported for other fungi (Bago et al., 2002). We then examined the thickness of the cell walls for three cell types using TEM. TEM showed that the chlamydospore-like cells had thicker cell walls than blastospores and pycnidiospores (Figure 5). We also found that pseudohyphae and the elongated suspensor cells, where chlamydospores are usually attached to the surrounding mycelium, have a cell wall thickness similar to pycnidiospores (Figure 5). No differences were observed for the chlamydospore-like cells produced by the 1A5 and 3D7 strains. On average, chlamydospore-like cells produced by *Z. tritici* had a cell wall thickness of ~460 nm, about four times thicker than the cell walls found in blastospores and pycnidiospores. Despite the thickness of the cell wall, we could not differentiate an extra cell wall layer as reported in chlamydospores from other fungal species (Fabry, Schmid, Schraps, &

Ansorg, 2003; Sitton & Cook, 1981).

The chlamydospore-like cells are metabolically active and highly stress tolerant. The chlamydospore-like cells of 1A5 germinated and produced hyphae. After 12 h of incubation on WA plates, we observed germ tubes emerging from the chlamydospore-like cells, which led to the development of hyphae at 24 hai (Figure 6B and C). Blastospores used as controls initially germinated from one apical side, generating the first and second germ tubes within 12 hai (Figure 6A). We inoculated wheat with chlamydospore-like cells from GFP-tagged 1A5 to observe by confocal microscopy whether these cells could germinate on the leaf surface. At 24 hpi, free chlamydospore-like cells and chlamydospore-like cells still attached to a suspensor cell produced germ tubes and hyphae on the surface of wheat leaves (Figure 6D). These results suggest that chlamydospore-like cells may be able to cause infections.

We also investigated whether chlamydospore-like cells share other characteristics of fungal resting spores, such as an ability to resist drought and temperature extremes. Incubation for one day under drought stress reduced viability of blastospores and pseudohyphae by 70%, while the chlamydospore-like cells had a reduction in cell viability of only 23% (Figure 7A). These rates changed little after 3 days of drought stress. After 5 days of drought stress, the survival rates were 10%, 19%, and 49% for blastospores, pseudohyphae and chlamydospore-like cells, respectively (Figure 7A). After 10 days of drought stress, the chlamydospore-like cells exhibited a survival rate of 50%, significantly higher than the other cell types (Figure 7A). In the cold stress

experiment, only the chlamydospore-like cells survived the cold shock, with no statistically significant difference in the survival rates of 23%, 17%, and 19% after 1 min, 2 min and 3 min in liquid nitrogen, respectively (Figure 7B). In the heat stress experiment, 30°C affected blastospores and chlamydospore-like cells equally, but the 35°C treatment killed all the blastospores while chlamydospore-like cells and pseudohyphae survived at rates of 12% and 6%, respectively (Figure 7C). None of the morphotypes survived at 40°C (Figure 7C). For all tested environmental stresses, chlamydospore-like cells were the morphotype that exhibited the highest survival rate, suggesting that this structure exhibits ecological characteristics typical for fungal resting spores that enable improved survival to different stresses encountered in nature.

Chlamydospore-like cells form on wheat plants during the infection process. Wheat plants were inoculated with pycnidiospores of all four strains and kept in a greenhouse chamber until pycnidia formation. Microscopic examination of the spore solution harvested from 20-day old infected leaves showed the presence of chlamydospore-like cells mixed among the pycnidiospores (Supplementary Figure S7). We observed free chlamydospore-like cells (Supplementary Figure S7A), as well as germinating chlamydospore-like cells (Supplementary Figure S7B), with some still attached to suspensor cells (Supplementary Figure S7B).

Germinating pycnidiospores produce blastospores on the surface of wheat leaves. Pycnidiospores of a GFP-tagged 3D7 strain were inoculated onto wheat plants and monitored using confocal microscopy. At 24 hai, we observed the expected

554 pycnidiospore germination and initial hyphal branching, but we also observed newly-
555 budding blastospores (Figure 8A). After 48 hours, there was an increase in the number
556 of budding points on germinated pycnidiospores, and an increase in the number of free
557 blastospores visible on the leaf (Figure 8B). This suggests that pycnidiospores of *Z.*
558 *tritici* can germinate to produce additional blastospores even before penetration of the
559 wheat leaf, providing an alternative mechanism for splash-dispersal of infective
560 propagules and potentially providing a substantial increase in the total inoculum load
561 associated with an infection cycle. At 48 hpi we also noticed many anastomosis events
562 between pycnidiospores and new blastospores (Figure 8B).
563
564 **DISCUSSION**
565 Fungi evolved to perceive a wide array of environmental signals and reprogram their
566 cellular responses accordingly in order to maximize their fitness. Though much research
567 has been oriented around morphological changes and their associated transcriptional
568 pathways in response to different stressors in fungal pathogens of humans (Biswas, Van
569 Dijck, & Datta, 2007; Klein & Tebbets, 2007; Noble et al., 2017), knowledge in this area
570 is limited for plant pathogens. Our study shows how different environments can affect
571 cellular morphologies in the wheat pathogen *Z. tritici*. We also demonstrate the
572 phenotypic plasticity of this fungus in response to environmental changes, as well as
573 differential responses to the same environments among strains. An unexpected
574 outcome of this study was the discovery of two novel morphotypes, one of which may
575 have important epidemiological implications.
576

We found that several environmental factors can affect morphological transitions in strain-specific ways for four natural *Z. tritici* strains sampled from the same Swiss population. All four strains switched to hyphal growth in a nutrient-poor minimal medium, suggesting that nutritional limitation may best simulate the conditions encountered by spores on the leaf surface. Morphological changes induced by limited nutrients has also been described in other dimorphic plant pathogenic fungi distributed across different phyla (Gauthier, 2015; Nadal et al., 2008). Nutrients are known to be present on the leaf surface in very small quantities and are usually surrounded by epicuticular waxes (Derridj, 1996). As a result, plant pathogens typically experience nutritient limitations while growing on leaves. It is thought that secreted enzymes, including plant cell wall degrading enzymes (PCWDEs) such as cutinases, are required to obtain nutritients during this stage of development, but *Z. tritici* has few PCWDEs compared to other fungi (Ohm et al., 2012), suggesting that the perception of a nutrient-limited environment may act as a stimulus to induce a switch to an exploratory morphotype (hyphae) that can better explore the environment for food. We found a significative increase in the frequency of anastomosis events during mycelium formation under nutrient-limited conditions. Mycelial networks formed by anastomosis enable a shared cytoplasmic flow that can more efficiently distribute water, nutrients, and signals within a fungal colony (Fleissner et al., 2005; Glass, Rasmussen, Roca, & Read, 2004). Moreover, hyphal fusions were shown to be required for virulence for some plant pathogens (Craven, Velez, Cho, Lawrence, & Mitchell, 2008; Prados Rosales & Di Pietro, 2008). We hypothesize that hyphal anastomosis provides benefits during epiphytic growth of germinating *Z. tritici* pycnidiospores prior to stomatal penetration, with anastomosis

600 facilitating colony establishment and increasing strain fitness during colonization of the
601 host.
602
603 The oxidative burst is a ubiquitous plant defense response to pathogen infection,
604 resulting in a rapid release of reactive oxygen species (ROS), including hydrogen
605 peroxide (H_2O_2) (Shetty et al., 2007). The ROS produced during plant defense were
606 proposed to have various functions, including activation of plant defense-related genes
607 and production of phytoalexins in addition to a direct antimicrobial effect that inhibits
608 pathogen growth (Fones & Preston, 2012; Lamb & Dixon, 1997; Yang et al., 2017).
609 Though many studies have demonstrated its antimicrobial effects, the effects of H_2O_2 on
610 morphological transitions remains largely unexplored. In *Candida albicans*, H_2O_2 induces
611 hyphal differentiation in a dose-dependent manner (Nasution et al., 2008). Our results
612 show that blastospores of three out of four *Z. tritici* strains switch to hyphae and
613 pseudohyphae when exposed to H_2O_2 in a dose-dependent manner. A cell density
614 dependence was also found. The different cell density responses suggest that the H_2O_2
615 is more rapidly metabolized by fungal hydroperoxidase proteins (catalases, peroxidases
616 and catalase-peroxidase), leading to lower toxicity at higher cell densities. Several
617 genes encoding peroxidases and catalase-peroxidases were identified in the genome of
618 *Z. tritici* (Levy, Eyal, & Hochman, 1992; Morais do Amaral, Antoniw, Rudd, & Hammond-
619 Kosack, 2012), which may explain the observed phenotype. The inability of 1A5 to
620 differentiate hyphae from blastospores at any H_2O_2 concentration suggests that this
621 strain either cannot sense oxidative stress or that it possesses a more efficient

622 antioxidant response that can neutralize the effects of H_2O_2. Further experiments will be
623 needed to test these hypotheses.
624
625 Fungal pathogens also need to be able to adapt to different pHs found in different
626 environments. pH is known to affect many physiological functions in fungi, including
627 growth and cell wall remodeling (Bignell, 2012). In *C. albicans*, a signaling pathway
628 controlling pH-responsive genes is regulated by the ambient pH, where an acidic pH
629 induces yeast-like growth and a neutral-alkaline pH favors formation of hyphae (Biswas
630 et al., 2007). Our results show that blastospores of *Z. tritici* respond differently to pH
631 than *C. albicans* yeast cells. Acidic pH did not affect the transition to hyphal growth
632 whereas alkaline pH repressed the formation of hyphae. The repression of hyphal
633 growth by alkaline pH was also reported for the dimorphic plant pathogen *Ustilago*
634 *maydis* (Ruiz-Herrera, Leon, Guevara-Olvera, & Carabez-Trejo, 1995). Alkaline pH not
635 only repressed the transition to hyphal growth in *Z. tritici*, but it also induced high
636 vacuolization of the blastospores. Changes in vacuole morphology and physiology have
637 been related to defects on hyphal growth and virulence in fungal pathogens of humans
638 and plants (Richards, Gow, & Veses, 2012; Veses & Gow, 2008). Therefore, the high
639 vacuolization by alkaline pH may explain the repression of hyphal growth observed in
640 this condition. pH responses remain poorly understood in the *Z. tritici*-wheat
641 pathosystem, but the leaf surface and apoplast colonized by *Z. tritici* during infection are
642 usually neutral-acidic environments (Edwards & Bowling, 1986). We hypothesize that *Z.*
643 *tritici* is better adapted to colonize an acidic pH environment than an alkaline
644 environment.

Temperature is an important abiotic factor that strongly affects growth, reproduction, and development in fungi (Lendenmann, Croll, Palma-Guerrero, Stewart, & McDonald, 2016; Ponomarenko, Goodwin, & Kema, 2011). Thermally dimorphic human fungal pathogens usually undergo morphological transitions in response to host temperature (Gauthier, 2015; Nemecek, Wüthrich, & Klein, 2006), but temperature has not been reported to affect the cell morphology of fungal plant pathogens. *Z. tritici* is the first plant pathogen shown to undergo morphological transitions after exposure to high temperatures (Lendenmann et al., 2016; Motteram et al., 2011). Our experiments showed that a change in temperature from 18°C to 27°C triggered hyphal growth in three out of four tested *Z. tritici* strains. For these three strains, an increase in hyphal elongation and formation of branches occured soon after exposure to the higher temperature. The hyphae formed at a high temperature appeared thicker than those formed under nutritient limitations and it is not clear if they would be able to cause infections.

We used transcriptome sequencing to identify genes associated with mycelial growth in *Z. tritici*. It was shown in other plant pathogenic fungi that starvation induces the expression of virulence-related genes (Coleman, Henricot, Arnau, & Oliver, 1997; Talbot, Ebbole, & Hamer, 1993). In *Z. tritici*, we found that genes relevant for virulence, including secreted hydrolytic proteins and candidate effectors, were upregulated in both hyphae-inducing conditions (carbon-depleted medium and *in planta*), suggesting that genes controlling morphogenesis and virulence may be co-regulated under nutrient-limited conditions. In *C. albicans,* genes related to hyphal growth are co-regulated by

668 transcription factors that affect expression of genes involved in virulence (Kumamoto &
669 Vinces, 2005; Thompson et al., 2011). However, it is important to note that not every
670 virulence function is connected to morphogenesis. The specific genes involved in the
671 activation and regulation of these morphological transitions remain unknown for *Z. tritici*.
672
673 An unexpected outcome of this study was the discovery of chlamydospore-like cells in *Z.*
674 *tritici.* The preponderance of evidence indicates that these cells are truly
675 chlamydospores. Their morphology matched the chlamydospores described in other
676 fungi: spherical, thick-walled cells with a high lipid content that form either intercalated or
677 at the ends of filamentous hyphae and occasionally on pseudohyphae (Lin & Heitman,
678 2005; Martin, Douglas, & Konopka, 2005). We also showed that these cells were able to
679 survive several stresses that killed other cell types, including dessication and high and
680 low temperatures, consistent with the function of chlamydospores as long-term survival
681 structures in other fungi (Couteaudier & Alabouvette, 1990; Lin & Heitman, 2005;
682 McNeel et al., 1983; Oliveira, Aguiar, Tessmann, Pujade-Renaud, & Vida, 2012). We
683 conclude that *Z. tritici* produces chlamydospores.
684
685 This is the first time that chlamydospores have been found in a plant pathogen that is
686 thought to mainly inhabit the phyllosphere. Though chlamydospores were especially
687 prominent in the 1A5 strain at high temperature, we observed chlamydospore production
688 in all four strains both *in vitro* and *in planta*. We hypothesize that the chlamydospores
689 produced by *Z. tritici* may contribute an important source of inoculum that can survive
690 between growing seasons and perhaps form a long-term spore-bank that can persist for

691 many years in wheat-growing regions. These properties could impact the management
692 of Septoria Tritici Blotch (STB), but additional studies will be needed to understand the
693 roles played by chlamydospores during the disease cycle of this pathogen.
694
695 Another finding with epidemiological implications was to demonstrate that blastospores
696 can form from germinating pycnidiospores on the surface of wheat leaves. This
697 possibility was proposed more than 30 years ago (Annone, 1987; Djerbi, 1977), but was
698 not followed up in subsequent studies. The formation of blastospores during *in vitro*
699 growth in nutrient-rich medium is why *Z. tritici* has long been considered to be a
700 dimorphic fungus. But until now it was not clear if the blastospores could also form on
701 leaf surfaces in nature. Our experiments confirmed that blastospores are produced
702 during a natural infection, but it remains unclear whether they make a significant
703 contribution to the development of epidemics. Given their small size and increasing
704 abundance over time, we hypothesize that they may play an important role in the
705 explosive increase in STB that can occur following prolonged rainy periods that last for
706 several days (Annone, 1987; Jones & LEE, 1974).
707
708 In conclusion, we demonstrate that *Z. tritici* responds morphologically to diverse
709 environmental stimuli, and we propose distinct biological roles for different morphotypes.
710 We also illustrate the advantage of including different natural strains when studying the
711 response of a species to environmental factors, as we found different morphological
712 responses among the tested strains. Our findings provide important new insights into the
713 *Z. tritici*-wheat pathosystem including: 1) the phenotypic plasticity of *Z. tritici* in response

714 to different environmental changes; 2) the reclassification of *Z. tritici* as a pleomorphic
715 fungus due to its ability to produce four distinct morphotypes; 3) the discovery of
716 chlamydospores that may help the fungus to survive stressful conditions; 4) the
717 formation of blastospores from germinating pycnidiospores on the surface of wheat
718 leaves, enabling a potentially significant increase in inoculum size. These findings
719 position *Z. tritici* as a good model organism to explore how morphological changes can
720 affect adaptation to different environments in fungal plant pathogens.
721
722 **ACKNOWLEDGEMENTS**
723 Carolina S. Francisco was supported by a PhD research fellowship from CAPES - Brazil
724 (process n° 002087/2015-04). We thank Andrea Sanchez-Vallet for providing the
725 fluorescent *Z. tritici* Swiss strains used in this study and for her critical reading of the
726 manuscript. We also thank Lukas Meile, Julien P. L. Alassimone, and Danilo A. Pereira
727 for discussions in the course of this work. RNA processing and sequencing were
728 performed in the Genetic Diversity Center (GDC) of ETH Zurich and the Genomics
729 Facility of ETH Basel, respectively. Transmission electron microscopy (TEM) and
730 confocal microscopy were performed at the Scientific Center for Optical and Electron
731 Microscopy (ScopeM) of ETH Zurich.
732
733
734 **REFERENCES**
735 Anders, S., Pyl, P. T., & Huber, W. (2015). HTSeq--a Python framework to work with
736 high-throughput sequencing data. *Bioinformatics, 31*(2), 166-169.
737 doi:10.1093/bioinformatics/btu638

Annone, J. (1987). *Observacion de conidios se cundarios de Septoria tritici Rob. ex Desm. por medio de impresiones foliareas*. Paper presented at the In: Kohli M. M. & van Beuningen L. T. (Eds.). In: Conferencia regional sobre la septoriosis del trigo, Montevideo, pp. 80-87.

Bago, B., Zipfel, W., Williams, R. M., Jun, J., Arreola, R., Lammers, P. J., . . . Shachar-Hill, Y. (2002). Translocation and utilization of fungal storage lipid in the arbuscular Mycorrhizal symbiosis. *Plant Physiology, 128*(1), 108-124. doi:10.1104/pp.010466

Bignell, E. (2012). The molecular basis of pH sensing, signaling, and homeostasis in fungi. *Advances in Applied Microbiology, 79*, 1-18. doi:10.1016/B978-0-12-394318-7.00001-2

Biswas, S., Van Dijck, P., & Datta, A. (2007). Environmental sensing and signal transduction pathways regulating morphopathogenic determinants of *Candida albicans*. *Microbiology and Molecular Biology Reviews, 71*(2), 348-376. doi:10.1128/MMBR.00009-06

Bolger, A. M., Lohse, M., & Usadel, B. (2014). Trimmomatic: a flexible trimmer for Illumina sequence data. *Bioinformatics, 30*(15), 2114-2120. doi:10.1093/bioinformatics/btu170

Bottcher, B., Pollath, C., Staib, P., Hube, B., & Brunke, S. (2016). Candida species rewired hyphae developmental programs for chlamydospore formation. *Frontiers in Microbiology, 7*, 1697. doi:10.3389/fmicb.2016.01697

Brand, A. (2012). Hyphal growth in human fungal pathogens and its role in virulence. *International Journal of Microbiology,* 1-11. doi:10.1155/2012/517529

Brown, A. J. P., Cowen, L. E., di Pietro, A., & Quinn, J. (2017). Stress Adaptation. *Microbiology Spectrum, 5*(4). doi:10.1128/microbiolspec.FUNK-0048-2016

Choi, Y. E., & Goodwin, S. B. (2011). Gene encoding a c-Type cyclin in *Mycosphaerella graminicola* is involved in aerial mycelium formation, filamentous growth, hyphal swelling, melanin biosynthesis, stress response, and pathogenicity. *Molecular Plant-Microbe Interactions, 24*(4), 469-477. doi:1094/MPMI-04-10-0090

Coleman, M., Henricot, B., Arnau, J., & Oliver, R. P. (1997). Starvation-induced genes of the tomato pathogen *Cladosporium fulvum* are also induced during growth in planta. *Molecular Plant-Microbe Interaction, 10*(9), 1106-1109. doi: 1094/MPMI.1997.10.9.1106

Cousin, A., Mehrabi, R., Guilleroux, M., Dufresne, M., T, V. D. L., Waalwijk, C., . . . Kema, G. H. (2006). The MAP kinase-encoding gene MgFus3 of the non-appressorium phytopathogen *Mycosphaerella graminicola* is required for penetration and *in vitro* pycnidia formation. *Molecular Plant Pathololology, 7*(4), 269-278. doi:10.1111/j.1364-3703.2006.00337.x

Couteaudier, Y., & Alabouvette, C. (1990). Survival and inoculum potential of conidia and chlamydospores of *Fusarium oxysporum* f.sp. *lini* in soil. *Canadian Journal of Microbiology, 36*(8), 551-556. doi:10.1139/m90-096

Craven, K. D., Velez, H., Cho, Y., Lawrence, C. B., & Mitchell, T. K. (2008). Anastomosis is required for virulence of the fungal necrotroph *Alternaria brassicicola*. *Eukaryotic Cell, 7*(4), 675-683. doi:10.1128/EC.00423-07

Croll, D., Zala, M., & McDonald, B. A. (2013). Breakage-fusion-bridge cycles and large insertions contribute to the rapid evolution of accessory chromosomes in a fungal pathogen. *PLoS Genetics, 9*(6), e1003567. doi:10.1371/journal.pgen.1003567

Derridj, S. (1996). Nutrients on the leaf surface. In: Morris C. E., Nicot P. C., & Nguyen-The C. (Eds.). *Aerial Plant Surface Microbiology* (pp. 25-42). New York: Plenum Press.

Djerbi, M. (1977). Épidémiologie du *Septoria tritici Rob. et Desm*. Conservation et mode de formation de l'inoculum primaire. *Société Française de Phytopathologie*, 91-101.

Edwards, J. A., Chen, C., Kemski, M. M., Hu, J., Mitchell, T. A., & Rappleye, C. A. (2013). Histoplasma yeast and mycelial transcriptomes reveals pathogenic-phase and lineage-specific gene expression profiles. *BMC Genomics, 14*(695), 1-19. doi: 10.1186/1471-2164-14-695

Edwards, M. C., & Bowling, D. J. F. (1986). The growth of rust germ tubes towards stomata in relation to pH gradients. *Physiological and Molecular Plant Pathology, 29*, 185-196. doi:10.1016/S0048-4059(86)80020-0

Fabry, W., Schmid, E. N., Schraps, M., & Ansorg, R. (2003). Isolation and purification of chlamydospores of *Candida albicans*. *Medical Mycology, 41*, 53-58. doi:10.1080/mmy.41.1.53.58

Fleissner, A., Sarkar, S., Jacobson, D. J., Roca, M. G., Read, N. D., & Glass, N. L. (2005). The so locus is required for vegetative cell fusion and postfertilization events in *Neurospora crassa*. *Eukaryotic Cell, 4*(5), 920-930. doi:10.1128/EC.4.5.920-930.2005

826 Fones, H., & Gurr, S. (2015). The impact of Septoria Tritici Blotch disease on wheat: An
827 EU perspective. *Fungal Genetics and Biology, 79*, 3-7.
828 doi:10.1016/j.fgb.2015.04.004
829
830 Fones, H., & Preston, G. M. (2012). Reactive oxygen and oxidative stress tolerance in
831 plant pathogenic Pseudomonas. *FEMS Microbiology Letters, 327*(1), 1-8.
832 doi:10.1111/j.1574-6968.2011.02449.x
833
834 Gancedo, J. M. (2001). Control of pseudohyphae formation in *Saccharomyces*
835 *cerevisiae*. *FEMS Microbioly Reviews, 25*, 107-123. doi:10.1111/j.1574-
836 6976.2001.tb00573.x
837
838 Gauthier, G. M. (2015). Dimorphism in fungal pathogens of mammals, plants, and
839 insects. *PLoS Pathogens, 11*(2), e1004608. doi:10.1371/journal.ppat.1004608
840
841 Glass, N. L., Rasmussen, C., Roca, M. G., & Read, N. D. (2004). Hyphal homing, fusion
842 and mycelial interconnectedness. *Trends in Microbiology, 12*(3), 135-141.
843 doi:10.1016/j.tim.2004.01.007
844
845 Grandaubert, J., Bhattacharyya, A., & Stukenbrock, E. H. (2015). RNA-seq based gene
846 annotation and comparative genomics of four fungal grass pathogens in the
847 genus Zymoseptoria identify novel orphan genes and species-specific invasions
848 of transposable elements. *G3 (Bethesda), 5*(7), 1323-1333.
849 doi:10.1534/g3.115.017731
850
851 Hoes, J. A. (1971). Development of chlamydospores in *Verticillium nigrescens* and
852 *Verticillium nubilum*. *Canadian Journal of Bonaty, 49*, 1863-1866.
853 doi:10.1139/b71-263
854
855 Hornby, J. M., Jacobitz-Kizzier, S. M., McNeel, D. J., Jensen, E. C., Treves, D. S., &
856 Nickerson, K. W. (2004). Inoculum size effect in dimorphic fungi: extracellular
857 control of yeast-mycelium dimorphism in *Ceratocystis ulmi*. *Applied and*
858 *Environmental Microbiology, 70*(3), 1356-1359. doi:10.1128/aem.70.3.1356-
859 1359.2004
860
861 Hornby, J. M., Jensen, E. C., Lisec, A. D., Tasto, J. J., Jahnke, B., Shoemaker, R., . . .
862 Nickerson, K. W. (2001). Quorum sensing in the dimorphic fungus *Candida*
863 *albicans* is mediated by farnesol. *Applied and Environmental Microbiology, 67*(7),
864 2982-2992. doi:10.1128/AEM.67.7.2982-2992.2001
865
866 Jones, D. G., & LEE, N. P. (1974). Production of secundary conidia by *Septoria tritici* in
867 culture. *Transactions British Mycological Society, 62*(1), 212-213.
868 doi:10.1016/S0007-1536(74)80025-2
869

Kema, G. H., Yu, D., Frits, H. J. R., Shaw, M. W., & Baayen, R. P. (1996). Histology of the pathogenesis of *Mycosphaerella graminicola* in wheat. *Biochemistry and Cell Biology, 86*, 777-786.

Kilaru, S., Schuster, M., Ma, W., & Steinberg, G. (2017). Fluorescent markers of various organelles in the wheat pathogen *Zymoseptoria tritici*. *Fungal Genetics and Biology, 105*, 16-27. doi:10.1016/j.fgb.2017.05.001

King, R., Urban, M., Lauder, R. P., Hawkins, N., Evans, M., Plummer, A., . . . Rudd, J. J. (2017). A conserved fungal glycosyltransferase facilitates pathogenesis of plants by enabling hyphal growth on solid surfaces. *PLoS Pathogens, 13*(10), e1006672. doi:10.1371/journal.ppat.1006672

Klein, B. S., & Tebbets, B. (2007). Dimorphism and virulence in fungi. *Current Opinion in Microbiology, 10*(4), 314-319. doi:10.1016/j.mib.2007.04.002

Kumamoto, C. A., & Vinces, M. D. (2005). Contributions of hyphae and hypha-co-regulated genes to *Candida albicans* virulence. *Cell Microbiology, 7*(11), 1546-1554. doi:10.1111/j.1462-5822.2005.00616.x

Lamb, C., & Dixon, R. A. (1997). The oxidative burst in plant disease resistance. *Annual Review of Plant Physiology and Molecular Biology, 48*, 251-275. doi:10.1146/annurev.arplant.48.1.251

Lendenmann, M. H., Croll, D., Palma-Guerrero, J., Stewart, E. L., & McDonald, B. A. (2016). QTL mapping of temperature sensitivity reveals candidate genes for thermal adaptation and growth morphology in the plant pathogenic fungus *Zymoseptoria tritici. Heredity (Edinb), 116*(4), 384-394. doi:10.1038/hdy.2015.111

Levy, E., Eyal, Z., & Hochman, A. (1992). Purification and characterization of a catalase-peroxidase from the fungus *Septoria tritici*. *Archives of Biochemistry and Biophysics, 296*(1), 321-327. doi:10.1016/0003-9861(92)90579-L

Lin, X., Alspaugh, J. A., Liu, H., & Harris, S. (2014). Fungal morphogenesis. *Cold Spring Harbor Perspectives in Medicine, 5*(2), a019679. doi:10.1101/cshperspect.a019679

Lin, X., & Heitman, J. (2005). Chlamydospore formation during hyphal growth in *Cryptococcus neoformans*. *Eukaryotic Cell, 4*(10), 1746-1754. doi:10.1128/EC.4.10.1746-1754.2005

Lübbehüsen, T. L., Nielsen, J., & McIntyre, M. (2003). Morphology and physiology of the dimorphic fungus *Mucor circinelloides* (syn. *M. racemosus*) during anaerobic growth. *Mycological Research, 107*(2), 223-230. doi:10.1017/s0953756203007299

Martin, S. W., Douglas, L. M., & Konopka, J. B. (2005). Cell cycle dynamics and quorum sensing in *Candida albicans* chlamydospores are distinct from budding and hyphal growth. *Eukaryotic Cell, 4*(7), 1191-1202. doi:10.1128/EC.4.7.1191-1202.2005

Mayer, F. L., Wilson, D., & Hube, B. (2013). *Candida albicans* pathogenicity mechanisms. *Virulence, 4*(2), 119-128. doi:10.4161/viru.22913

McNeel, D. J., Kulkarni, R. K., & Nickerson, K. W. (1983). Pleomorphism in *Ceratocystis ulmi*: chlamydospore formation. *Canadian Journal of Botany, 61*(5), 1349-1352. doi:10.1139/b83-143

Mehrabi, R., Ben M'Barek, S., van der Lee, T. A., Waalwijk, C., de Wit, P. J., & Kema, G. H. (2009). G(alpha) and Gbeta proteins regulate the cyclic AMP pathway that is required for development and pathogenicity of the phytopathogen *Mycosphaerella graminicola. Eukaryotic Cell, 8*(7), 1001-1013. doi:10.1128/EC.00258-08

Mehrabi, R., & Kema, G. H. (2006). Protein kinase A subunits of the ascomycete pathogen *Mycosphaerella graminicola* regulate asexual fructification, filamentation, melanization and osmosensing. *Molecular Plant Pathology, 7*(6), 565-577. doi:10.1111/j.1364-3703.2006.00361.x

Mehrabi, R., van der Lee, T., Waalwijk, C., & Kema, G. H. (2006). MgSlt2, a cellular integrity MAP kinase gene of the fungal wheat pathogen *Mycosphaerella graminicola*, is dispensable for penetration but essential for invasive growth. *Molecular Plant-Microbe Interactions, 19*(4), 389-398. doi:1094/MPMI-19-0389

Mehrabi, R., Zwiers, L. H., de Waard, M. A., & Kema, G. H. (2006). MgHog1 regulates dimorphism and pathogenicity in the fungal wheat pathogen *Mycosphaerella graminicola*. *Molecular Plant-Microbe Interactions, 19*(11), 1262-1269. doi:10.1094/MPMI-19-1262

Meile, L., Croll, D., Brunner, P. C., Plissonneau, C., Hartmann, F. E., McDonald, B. A., & Sanchez-Vallet, A. (2018). A fungal avirulence factor encoded in a highly plastic genomic region triggers partial resistance to Septoria Tritici Blotch. *New Phytologist, 219,* 1048-1061. doi:10.1111/nph.15180

Mirzadi Gohari, A., Mehrabi, R., Robert, O., Ince, I. A., Boeren, S., Schuster, M., . . . Kema, G. H. (2014). Molecular characterization and functional analyses of ZtWor1, a transcriptional regulator of the fungal wheat pathogen *Zymoseptoria tritici*. *Molecular Plant Pathology, 15*(4), 394-405. doi:10.1111/mpp.12102

Miyaji, M., Sano, A., & Sharmin, S. (2003). The role of chlamydospores of *Paracoccidioides brasiliensis*. *Japanese Journal of Medical Mycology, 44*, 133-138. doi:10.3314/jjmm.44.133

Mohammadi, N., Mehrabi, R., Mirzadi Gohari, A., Mohammadi Goltapeh, E., Safaie, N., & Kema, G. H. J. (2017). The ZtVf1 transcription factor regulates development and virulence in the foliar wheat pathogen *Zymoseptoria tritici*. *Fungal Genetics and Biology, 109*, 26-35. doi:10.1016/j.fgb.2017.10.003

Morais do Amaral, A., Antoniw, J., Rudd, J. J., & Hammond-Kosack, K. E. (2012). Defining the predicted protein secretome of the fungal wheat leaf pathogen *Mycosphaerella graminicola*. *PLoS One, 7*(12), e49904. doi:10.1371/journal.pone.0049904

Motteram, J., Lovegrove, A., Pirie, E., Marsh, J., Devonshire, J., van de Meene, A., . . . Rudd, J. J. (2011). Aberrant protein N-glycosylation impacts upon infection-related growth transitions of the haploid plant-pathogenic fungus *Mycosphaerella graminicola*. *Molecular Microbiology, 81*(2), 415-433. doi:10.1111/j.1365-2958.2011.07701.x

Nadal, M., Garcia-Pedrajas, M. D., & Gold, S. E. (2008). Dimorphism in fungal plant pathogens. *FEMS Microbiology Letters, 284*(2), 127-134. doi:10.1111/j.1574-6968.2008.01173.x

Nasution, O., Srinivasa, K., Kim, M., Kim, Y. J., Kim, W., Jeong, W., & Choi, W. (2008). Hydrogen peroxide induces hyphal differentiation in *Candida albicans*. *Eukaryotic Cell, 7*(11), 2008-2011. doi:10.1128/EC.00105-08

Nemecek, J. C., Wüthrich, M., & Klein, B. S. (2006). Global control of dimorphism and virulence in fungi. *Science, 312*, 583-588. doi:10.1126/science.1124105

Nigg, M., Laroche, J., Landry, C. R., & Bernier, L. (2015). RNAseq analysis highlights specific transcriptome signatures of yeast and mycelial growth phases in the Dutch Elm Disease fungus *Ophiostoma* novo-*ulmi*. *G3 (Bethesda), 5*(11), 2487-2495. doi:10.1534/g3.115.021022

Noble, S. M., Gianetti, B. A., & Witchley, J. N. (2017). *Candida albicans* cell-type switching and functional plasticity in the mammalian host. *Nature Reviews Microbiology, 15*(2), 96-108. doi:10.1038/nrmicro.2016.157

Ohm, R. A., Feau, N., Henrissat, B., Schoch, C. L., Horwitz, B. A., Barry, K. W., . . . Grigoriev, I. V. (2012). Diverse lifestyles and strategies of plant pathogenesis encoded in the genomes of eighteen Dothideomycetes fungi. *PLoS Pathogens, 8*(12), e1003037. doi:10.1371/journal.ppat.1003037

Oliveira, R. R., Aguiar, B. M., Tessmann, D. J., Pujade-Renaud, V., & Vida, J. B. (2012). Chlamydospores formation by *Corynespora cassiicola*. *Tropical Plant Pathology, 37*(6), 415-418. doi:10.1590/S1982-56762012000600006

Palma-Guerrero, J., Ma, X., Torriani, S. F., Zala, M., Francisco, C. S., Hartmann, F. E., . . . McDonald, B. A. (2017). Comparative transcriptome analyses in *Zymoseptoria tritici* reveal significant differences in gene expression among strains during plant infection. *Molecular Plant-Microbe Interactions, 30*(3), 231-244. doi:10.1094/MPMI-07-16-0146-R

Plissonneau, C., Hartmann, F. E., & Croll, D. (2018). Pangenome analyses of the wheat pathogen *Zymoseptoria tritici* reveal the structural basis of a highly plastic eukaryotic genome. *BMC Biology, 16*(1), 5. doi:10.1186/s12915-017-0457-4

Ponomarenko, A., Goodwin, S. B., & Kema, G. H. J. (2011). Septoria Tritici Bloch (STB of wheat. *Plant Health Instructor*. doi:10.1094/PHI-I-2011-0407-1001

Prados Rosales, R. C., & Di Pietro, A. (2008). Vegetative hyphal fusion is not essential for plant infection by *Fusarium oxysporum*. *Eukaryotic Cell, 7*(1), 162-171. doi:10.1128/EC.00258-07

Richards, A., Gow, N. A., & Veses, V. (2012). Identification of vacuole defects in fungi. *Journal of Microbiological Methods, 91*(1), 155-163. doi:10.1016/j.mimet.2012.08.002

Robinson, M. D., McCarthy, D. J., & Smyth, G. K. (2010). edgeR: a Bioconductor package for differential expression analysis of digital gene expression data. *Bioinformatics, 26*(1), 139-140. doi:10.1093/bioinformatics/btp616

Robinson, M. D., & Oshlack, A. (2010). A scaling normalization method for differential expression analysis of RNA-seq data. *Genome Biology, 11*(3), R25. doi:10.1186/gb-2010-11-3-r25

Ruiz-Herrera, J., Leon, C. G., Guevara-Olvera, L., & Carabez-Trejo, A. (1995). Yeast-mycelial dimorphism of haploid and diploid strains of *Ustilago maydis*. *Microbiology, 141*, 695-703. doi:10.1099/13500872-141-3-695

Schade, D., Walther, A., & Wendland, J. (2003). The development of a transformation system for the dimorphic plant pathogen *Holleya sinecauda* based on *Ashbya gossypii* DNA elements. *Fungal Genetics and Biology, 40*(1), 65-71. doi:10.1016/s1087-1845(03)00064-1

Shetty, N. P., Mehrabi, R., Lutken, H., Haldrup, A., Kema, G. H., Collinge, D. B., & Jorgensen, H. J. (2007). Role of hydrogen peroxide during the interaction

between the hemibiotrophic fungal pathogen *Septoria tritici* and wheat. *New Phytolologist, 174*(3), 637-647. doi:10.1111/j.1469-8137.2007.02026.x

Sitton, J. W., & Cook, R. J. (1981). Comparative mophology and survival of chlamydospore of *Fusarium roseum* 'Culmorum' and 'Graminearum'. *Ecology and Epidemiology, 71*(1), 85-90.

Son, H., Lee, J., & Lee, Y. W. (2012). Mannitol induces the conversion of conidia to chlamydospore-like structures that confer enhanced tolerance to heat, drought, and UV in *Gibberella zeae*. *Microbiological Research, 167*(10), 608-615. doi:10.1016/j.micres.2012.04.001

Steinberg, G. (2015). Cell biology of *Zymoseptoria tritici*: Pathogen cell organization and wheat infection. *Fungal Genetics and Biology, 79*, 17-23. doi:10.1016/j.fgb.2015.04.002

Talbot, N. J., Ebbole, D. J., & Hamer, J. E. (1993). Identification and characterization of MPGI, a gene involved in pathogenicity from the Rice Blast fungus *Magnaporthe grisea*. *The Plant Cell, 5*, 1575-1590. doi:10.1105/tpc.5.11.1575

Thompson, D. S., Carlisle, P. L., & Kadosh, D. (2011). Coevolution of morphology and virulence in Candida species. *Eukaryotic Cell, 10*(9), 1173-1182. doi:10.1128/EC.05085-11

Torriani, S. F., Melichar, J. P., Mills, C., Pain, N., Sierotzki, H., & Courbot, M. (2015). *Zymoseptoria tritici*: A major threat to wheat production, integrated approaches to control. *Fungal Genetics and Biology, 79*, 8-12. doi:10.1016/j.fgb.2015.04.010

Trapnell, C., Pachter, L., & Salzberg, S. L. (2009). TopHat: discovering splice junctions with RNA-Seq. *Bioinformatics, 25*(9), 1105-1111. doi:10.1093/bioinformatics/btp120

Veses, V., & Gow, N. A. (2008). Vacuolar dynamics during the morphogenetic transition in *Candida albicans*. *FEMS Yeast Research, 8*(8), 1339-1348. doi:10.1111/j.1567-1364.2008.00447.x

Veses, V., & Gow, N. A. (2009). Pseudohypha budding patterns of *Candida albicans*. *Medical Mycology, 47*(3), 268-275. doi:10.1080/13693780802245474

Vogel, H. J. (1956). A convenient growth medium for Neurospora (medium N). *Microbial Genetics Bulletin, 13*, 42-43.

Wang, L., & Lin, X. (2012). Morphogenesis in fungal pathogenicity: shape, size, and surface. *PLoS Pathogens, 8*(12), e1003027. doi:10.1371/journal.ppat.1003027

Wedge, M. E., Naruzawa, E. S., Nigg, M., & Bernier, L. (2016). Diversity in yeast-mycelium dimorphism response of the Dutch Elm disease pathogens: the inoculum size effect. *Canadian Journal of Microbiology, 62*(6), 525-529. doi:10.1139/cjm-2015-0795

Wickham, H. (2009). *ggplot2: Elegant Graphics for Data Analysis*. (2nd Ed,). New York: Use R. Springer-Verlag.

Yang, C., Li, W., Cao, J., Meng, F., Yu, Y., Huang, J., . . . Liu, J. (2017). Activation of ethylene signaling pathways enhances disease resistance by regulating ROS and phytoalexin production in rice. The *Plant Journal, 89*(2), 338-353. doi:10.1111/tpj.13388

Yemelin, A., Brauchler, A., Jacob, S., Laufer, J., Heck, L., Foster, A. J., . . . Thines, E. (2017). Identification of factors involved in dimorphism and pathogenicity of *Zymoseptoria tritici*. *PLoS One, 12*(8), e0183065. doi:10.1371/journal.pone.0183065

Zala, M., Mikaberidze, A., Alassimone, J. P. L., Muhammad, A., McDonald, B. A., & Sánchez-Vallet, A. (2018). Co-infection alters virulence dynamics in the wheat pathogen *Zymoseptoria tritici*. *in submission*.

Zhan, J., Linde, C. C., Jurgens, T., Merz, U., Steinebrunner, F., & McDonald, B. A. (2005). Variation for neutral markers is correlated with variation for quantitative traits in the plant pathogenic fungus *Mycosphaerella graminicola*. *Molecular Ecology, 14*(9), 2683-2693. doi:10.1111/j.1365-294X.2005.02638.x

Data Accessibility

All raw sequencing data were deposited into the NCBI Short Read Archive under the accession number SRP152081.

Author contributions

C.S.F. and J.P.-G. conceived and designed experiments. C.S.F., MMZ and J.P.-G. performed experiments. X.M. and C.S.F. were responsible for the bioinformatics analysis. C.S.F., B.A.M. and J.P.-G. wrote the paper.

Figure Legends

Figure 1. Effect of temperature on the cell morphology of four *Zymoseptoria tritici* strains. (A) Blastospores incubated on nutrient-rich YSB medium at 18°C (the control environment) multiply by budding as blastospores (white triangles). (B) The effect of high temperatures on *Z. tritici* morphology was observed by exposing the strains to 27°C. At 8 hours after incubation (hai) at the high temperature, blastospores of the 1E4 strain were faster to respond to the new environment by switching to filamentous growth. Black triangles point to hyphal branches. (C) At 24 hai, blastospores of the 3D1 and 3D7 strains began growing as hyphae. The 1A5 strain produced swollen cells (black arrows) and pseudohyphae (asterisks), without any evidence of hyphal differentiation. (D) At 48 hai, hyphal branches were abundant for the 1E4, 3D1, and 3D7 strains. The 1A5 strain continued to produce only swollen structures (black arrows). (E) At 96 hai, filamentous growth was observed for the 1E4, 3D1, and 3D7 strains. For the 1A5 strain, high temperature promoted the formation of two new morphotypes: pseudohyphae (asterisks) and chlamydospore-like cells (black arrows). (F) After 144 hours of incubation, the formation of chlamydospore-like cells was observed mainly at the tips of pseudohyphae for the 1A5 strain and at the distal ends of mycelial filaments for the remaining strains (1E4, 3D1, and 3D7) (black arrows). Bars represent 10 µm.

Figure. 2. Effect of carbon limitation on the cell morphology of four *Zymoseptoria tritici* strains. A nutrient-rich medium (YSB) and a carbon-depleted medium (Minimal Media without sucrose) were used to monitor the growth form transitions (A) Blastospores

incubated on YSB continued to multiply as budding blastospores and were used as controls. (B) Under carbon limitation stress, the blastospores of all tested strains began growing as hyphae after 24 hours of incubation (arrows). (C) At 144 hai, a mycelial growth was predominant, with frequent vegetative cell fusion events (asterisks) among hyphae. Bars represent 20 µm.

Figure. 3. Transcriptome signatures of blastospore and mycelial growth phases organized based on enrichment of molecular functional terms. (A) Common upregulated genes during blastospore growth among the *Zymoseptoria tritici* strains. (B) Common upregulated genes for mycelial growth among the *Z. tritici* strains.

Figure. 4. Staining of cell wall chitin and lipid content in the different morphotypes of *Zymoseptoria tritici.* Cell walls were stained with the chitin-binding dye Calcofluor White (blue color) and the lipid droplets were stained with Nile Red (red color). Blastospores, hyphae, and pseudohyphae showed a weaker fluorescence for Calcofluor White compared to chlamydospores (A), including those formed terminally (B) or intercalarily (C) via suspensor cells. A high accumulation of lipid droplets was observed in chlamydospores, as well as in blastospores and pseudohyphae. Hyphae only showed a high accumulation of lipid droplets in the hyphal branching zone. Bars represent 10 µm.

Figure. 5. Chlamydospore cells produced by *Zymoseptoria tritici* have thicker cell walls than pycnidiospores and blastospores. Black triangles point to a detaching daughter cell

1174 budding from a blastospore mother cell. Images were obtained by transmission electron
1175 microscopy. Two different magnifications are shown for eah morphotype: up panels
1176 scale bar = 2000 nm (low magnification), low panels scale bar = 500nm (high
1177 magnification).
1178
1179 **Figure. 6.** Chlamydospores produced by *Zymoseptoria tritici* are able to germinate both
1180 *in vitro* and on the surface of wheat leaves. (A) Blastospores were used as a control.
1181 Apical germination and hyphal elongation were observed after 12 hours of incubation on
1182 water agar (WA) plates at 18°C. At 24 hai, blastosporulation was observed from the
1183 germinated blastospores. (B) Terminal chlamydospores formed via suspensor cells and
1184 (C) free-chlamydospores initiated the germination after 12 h of incubation on water agar.
1185 Hyphal elongation was obvious at 24 h. Bars represent 10 μm. (D) Free-
1186 chlamydospores (upper image) and terminal chlamydospores (lower image) expressing
1187 cytoplasmic GFP (green color) produced germ tubes on the surface of wheat leaves
1188 after 24 hours of infection. Blue color corresponds to the autofluorescence detected from
1189 chlorophyll A. Asterisks indicate the suspensor cells where chlamydospores are
1190 attached. Bars represent 8 μm.
1191
1192 **Figure 7.** Chlamydospores produced by *Zymoseptoria tritici* are more tolerant to stress
1193 than blastospores and pseudohyphae. Survival rate (%) was estimated based upon the
1194 number of colonies formed after exposure to the stressful environment compared to the
1195 number of colonies formed in the control environment after seven days. (A)

Blastospores, pseudohyphae and chlamydospore cells were kept for 1, 3, 5, and 10 days in a sealed box containing anhydrous silica gel to produce a dry environment. This simulated drought stress affected blastospore and pseudohyphae survival over time. Chlamydospores were less affected and exhibited a survival rate of 50% after 10 days under drought stress. (B) The same three morphotypes were subjected to a cold shock. Blastospores, pseudohyphae, and chlamydospores were submerged in liquid nitrogen for 1, 2, and 3 minutes at -196 °C. Only chlamydospores survived this cold stress. (C) The same three morphotypes were subjected to heat stress based on incubation for 24 hours at 30°C, 35°C or 40°C. Blastospores and chlamydospores were equally affected at 30°C. The incubation at 35°C killed all the blastospores, while chlamydospore survived at a 12% rate, double the rate observed for pseudohyphae (6%). No colonies were observed after incubation at 40°C. One star indicates that the adjusted p value is under 0.05, two stars indicates that the p value is under 0.005, and three stars indicates that the p value is under 0.0005. NS indicates no significant difference.

Figure 8. Germinated pycnidiospores of *Zymoseptoria tritici* produce new blastospores via blastosporulation on the surface of wheat leaves. (A) At 24 hours after infection, pycnidiospores (asterisk) germinated and formed hyphal branches expressing GFP (green color). The germinated pycnidiospores produced new blastospores on the host leaves (arrow). (B) We observed a significant increase of budding points on germinated pycnidiospores (arrows), as well as more free blastospores on the leaf surface at 48 hours after infection. At this time point, we also observed several vegetative cell fusion

1218 events between blastospores and pycnidiospores, which are characterized by a tubular
1219 shaped bridge between the fusing cells (asterisks). Blue color corresponds to
1220 autofluorescence detected from Chlorophyll A. Bars represent 10 μm.

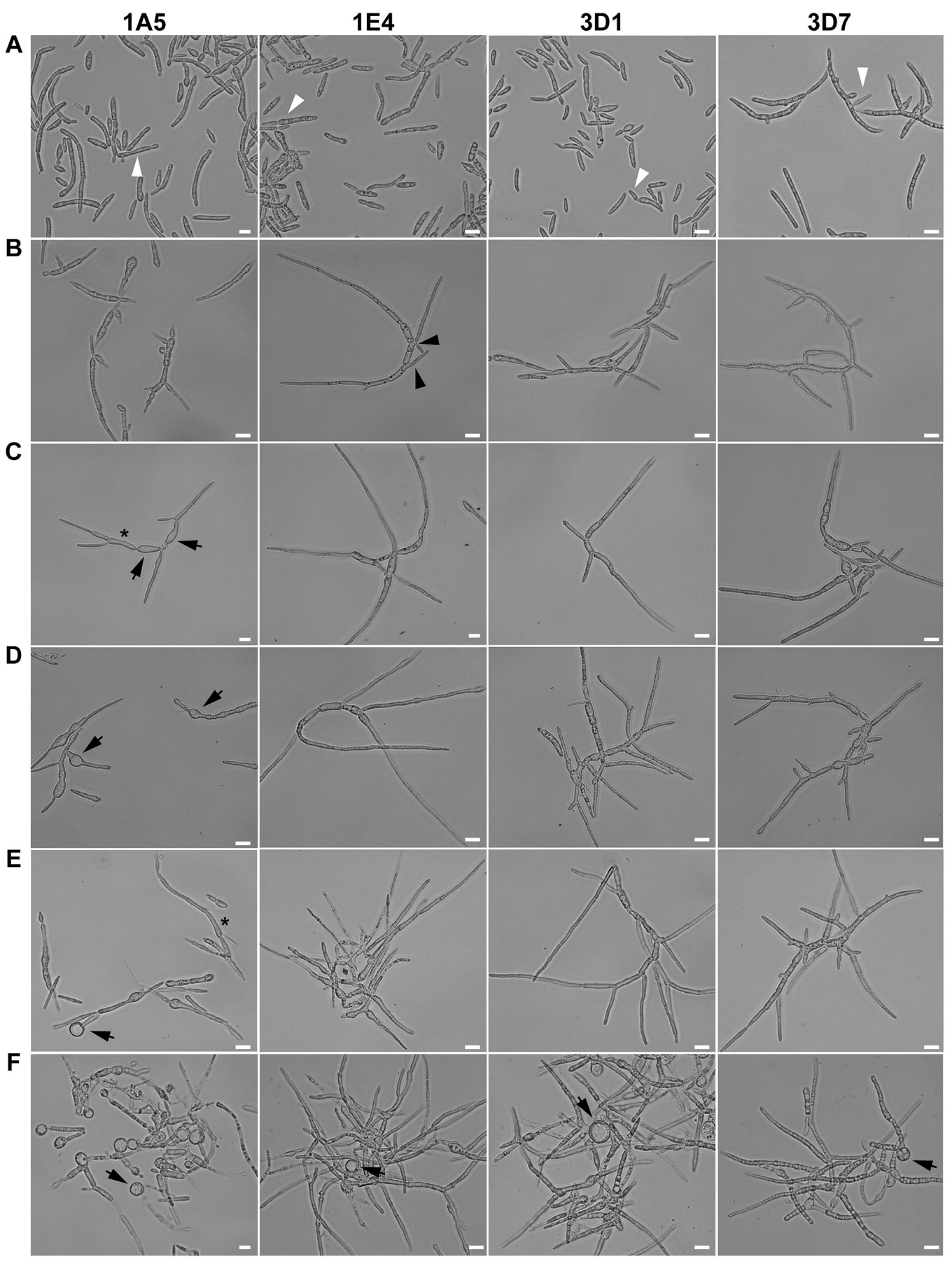
1A5
1E4
3D1
3D7
A
B
C
D
E
F

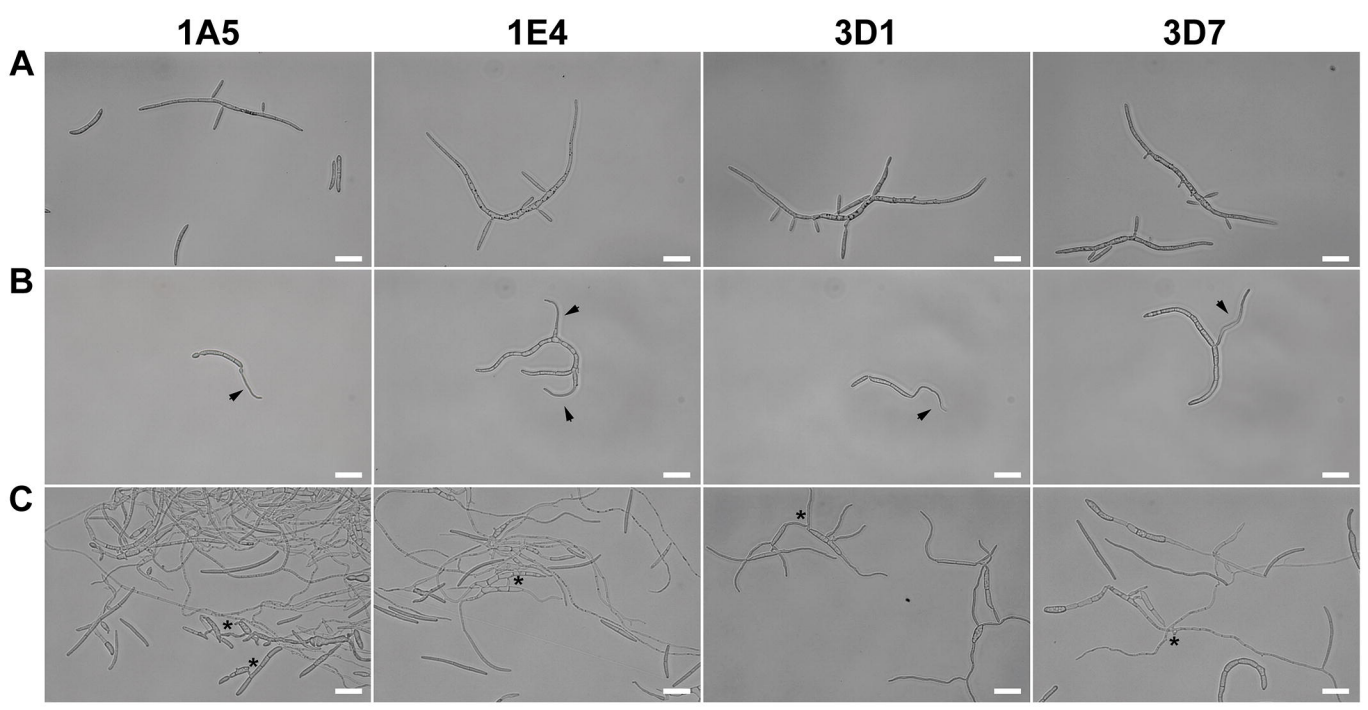
1A5
1E4
3D1
3D7
A
B
C

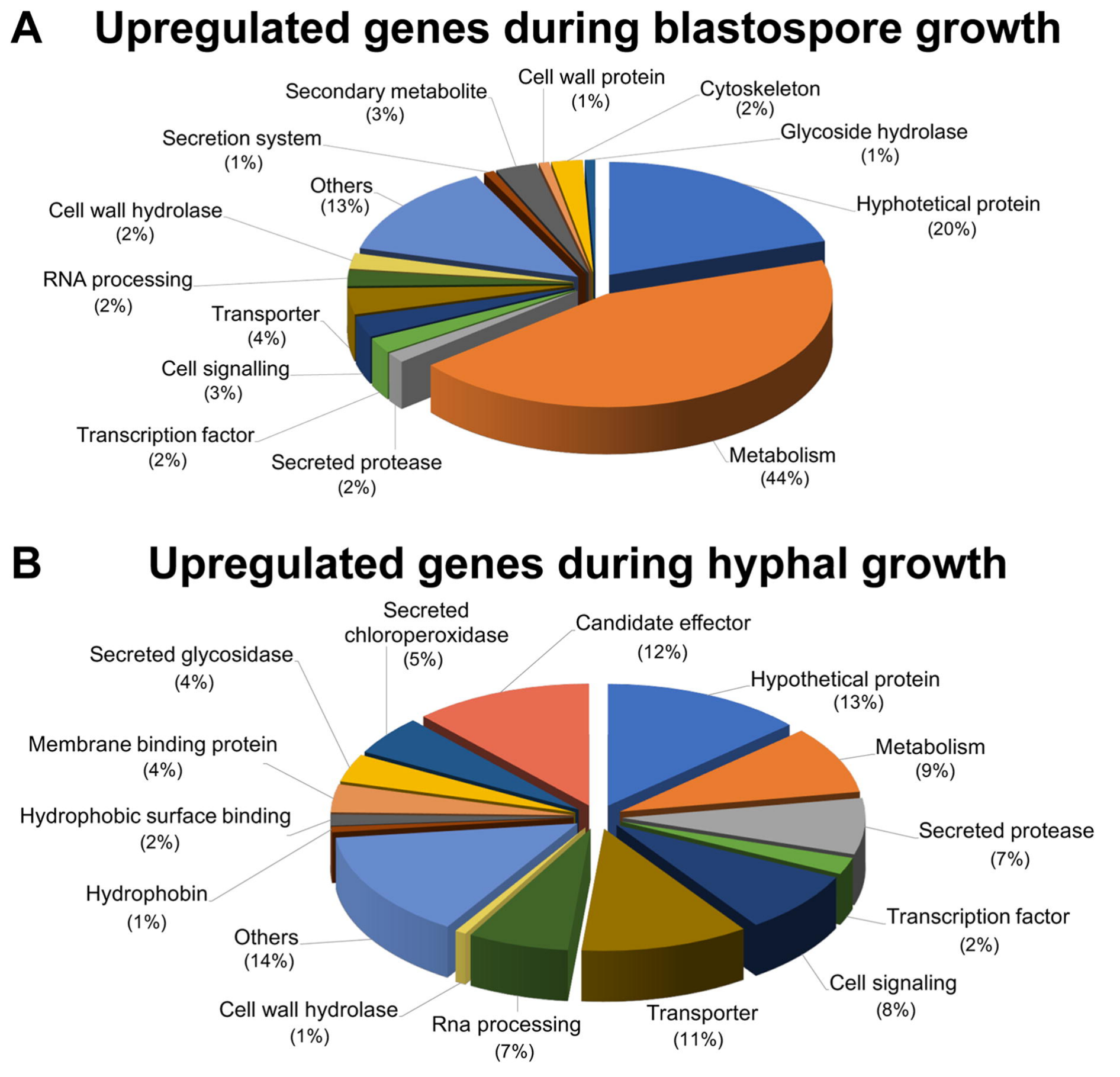
A Upregulated genes during blastospore growth
Secondary metabolite (3%)
Cell wall protein (1%)
Cytoskeleton (2%)
Glycoside hydrolase (1%)
Secretion system (1%)
Others (13%)
Hyphotetical protein (20%)
Cell wall hydrolase (2%)
RNA processing (2%)
Transporter (4%)
Cell signalling (3%)
Transcription factor (2%)
Secreted protease (2%)
Metabolism (44%)
B Upregulated genes during hyphal growth
Secreted chloroperoxidase (5%)
Candidate effector (12%)
Secreted glycosidase (4%)
Hypothetical protein (13%)
Membrane binding protein (4%)
Metabolism (9%)
Hydrophobic surface binding (2%)
Secreted protease (7%)
Hydrophobin (1%)
Transcription factor (2%)
Others (14%)
Cell signaling (8%)
Cell wall hydrolase (1%)
Rna processing (7%)
Transporter (11%)

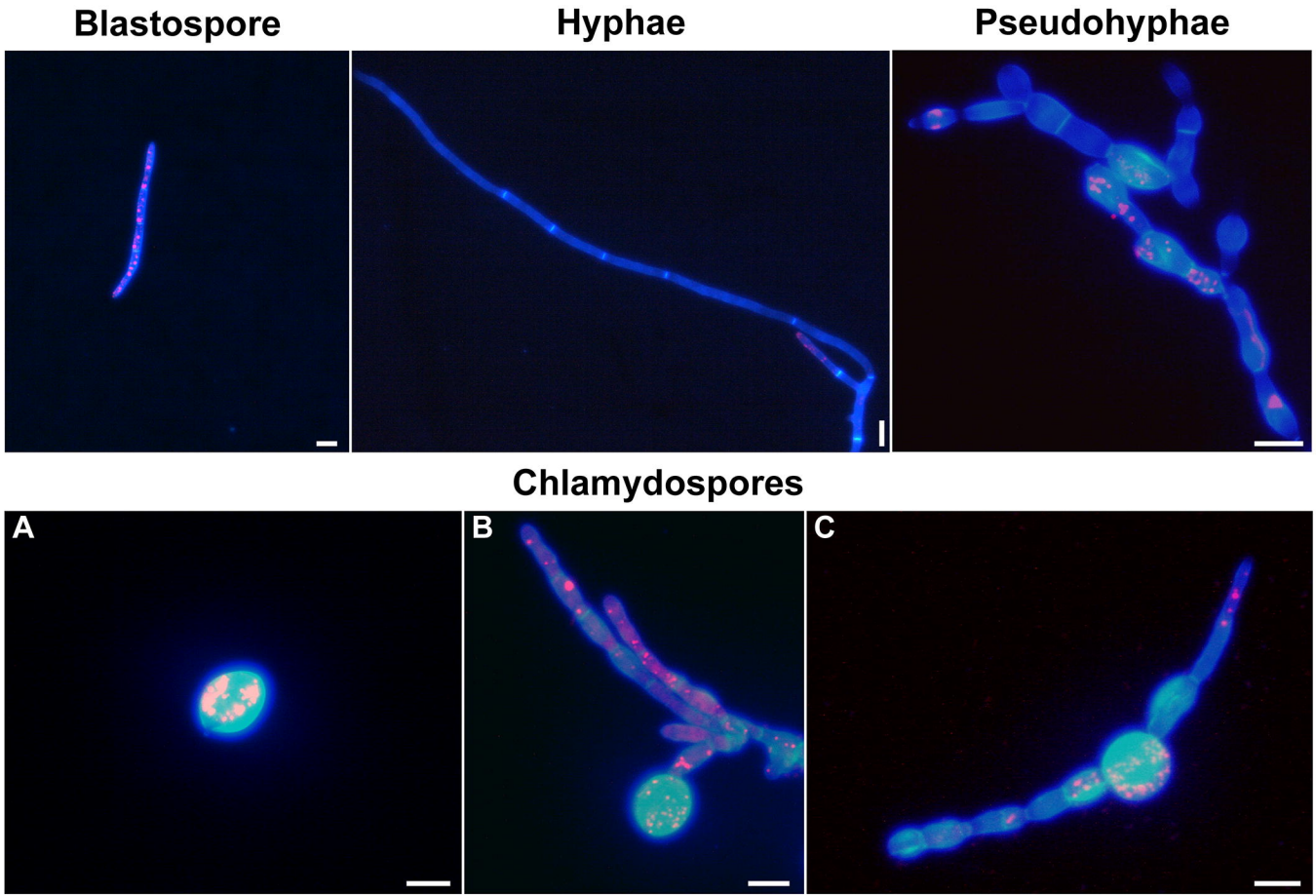
Blastospore
Hyphae
Pseudohyphae
Chlamydospores
A
B
C

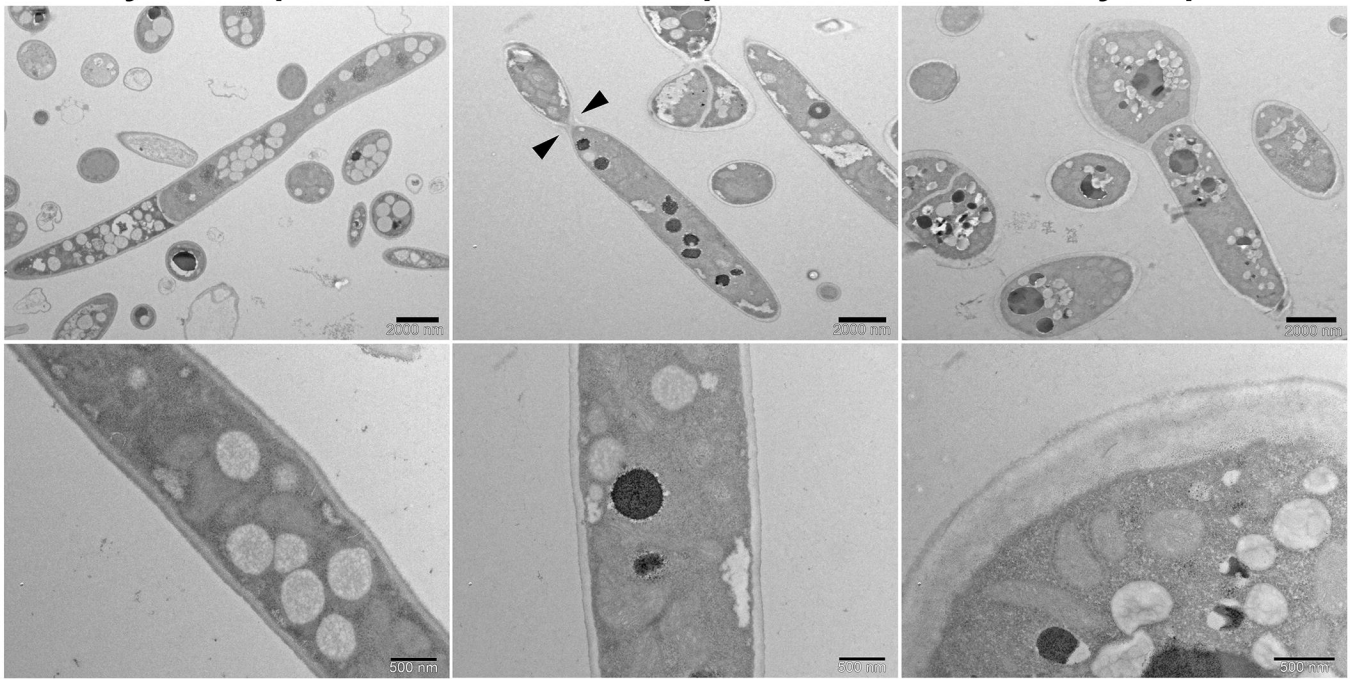
Pycnidiospore
Blastospore
Chlamydospore
2000 nm
2000 nm
2000 nm
500 nm
500 nm
500 nm

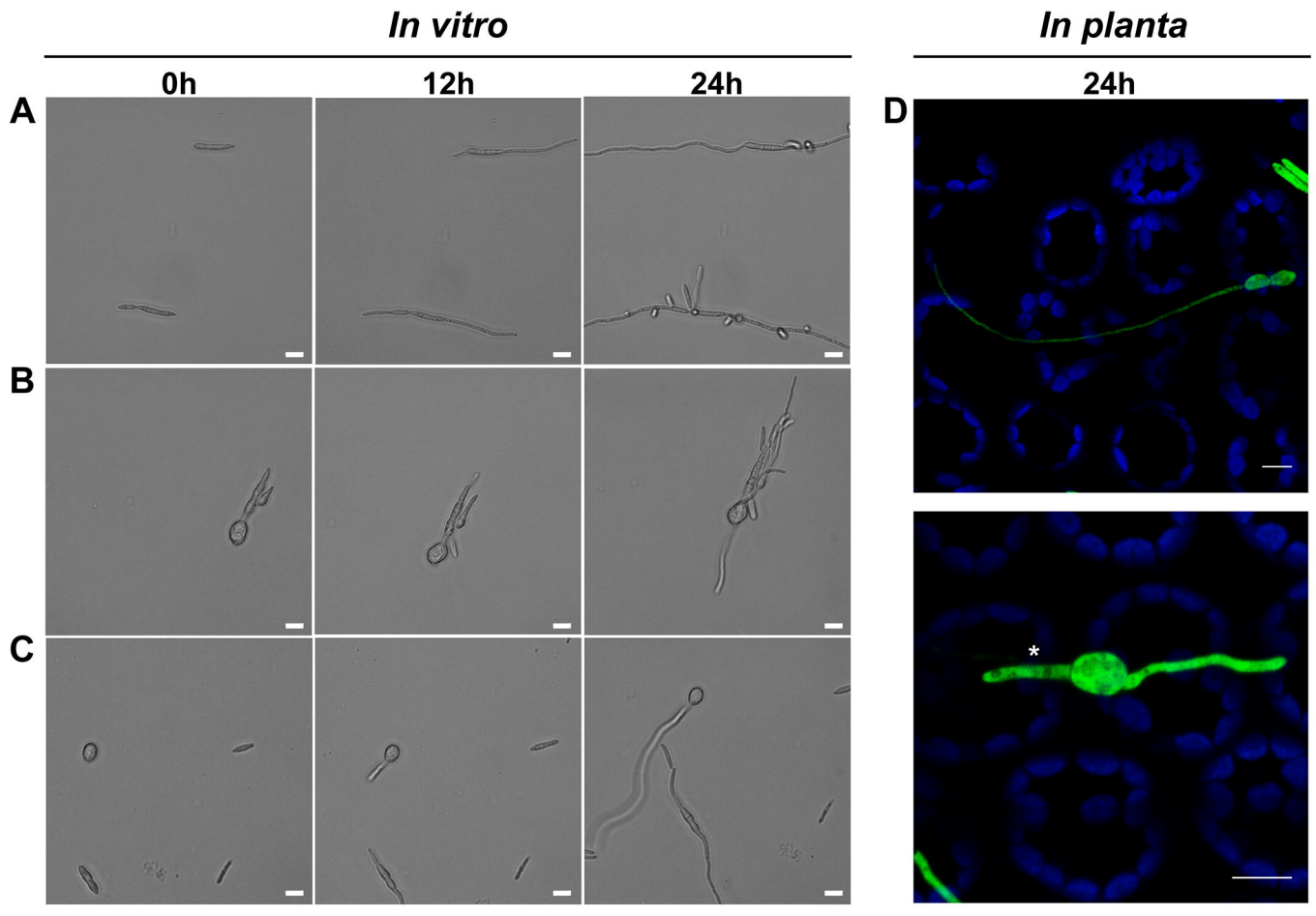
In vitro
In planta
0h
12h
24h
24h
A
B
C
D
*


A
Drought
B
Cold stress
C
Heat stress
Survival rate (%)
100
75
50
25
0
1d
3d
5d
10d
1min
2min
3min
30°C
35°C
40°C
Chlamydospore
Blastospore
Pseudohyphae
**
**
*
*
*
*
***
***
NS

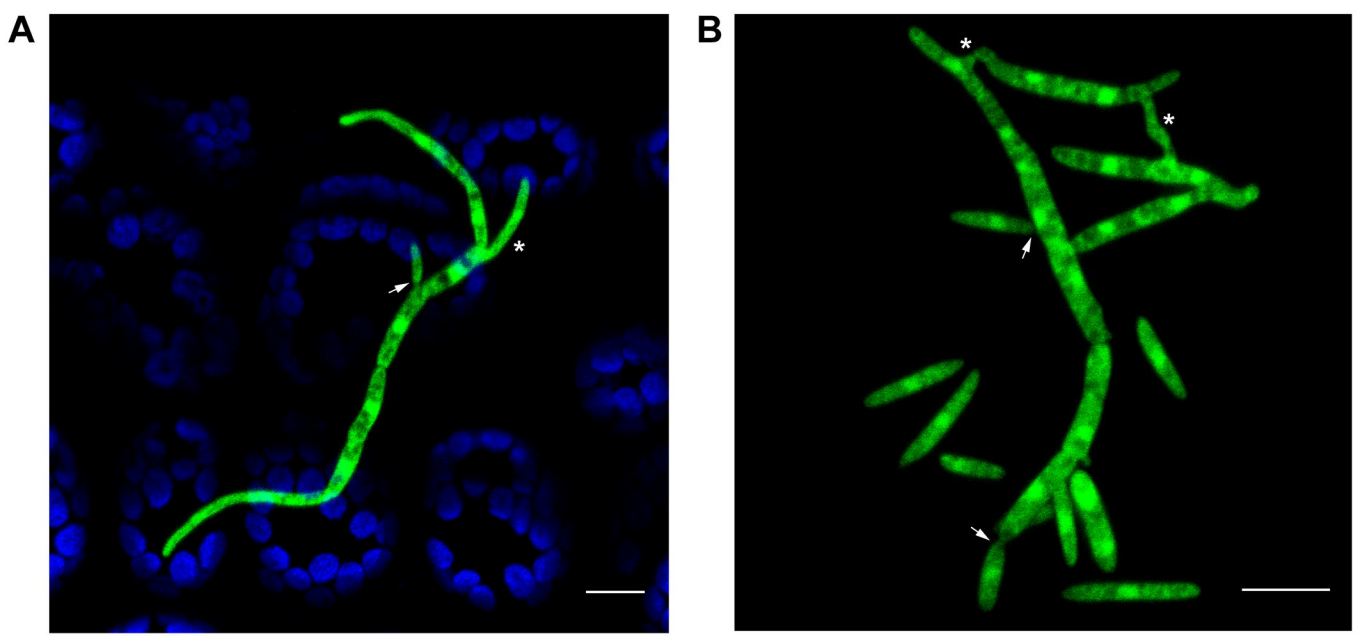
A
B